Available online at www.sciencedirect.com
SCIENCE DIRECT®

ELSEVIER

Journal of Chromatography A, 1000 (2003) 69–108

JOURNAL OF CHROMATOGRAPHY A

www.elsevier.com/locate/chroma

Review

Comprehensive two-dimensional gas chromatography: a powerful and versatile analytical tool

Jens Dallüge*, Jan Beens, Udo A.Th. Brinkman

Vrije Universiteit, Department of Analytical Chemistry and Applied Spectroscopy, de Boelelaan 1083, 1081 HV Amsterdam, The Netherlands

Abstract

Comprehensive two-dimensional gas chromatography (GC×GC) is a novel technique which is rapidly gaining importance for the analysis of complex samples. In the present review, attention is devoted to the principle and advantages, and main characteristics such as modulation, column combinations, detector requirements and data processing, of the technique. Specifically, GC×GC of a variety of real-life samples is discussed to demonstrate the applicability of the technique, with emphasis on the usefulness of the ordered-structure principle and on the analyte-identification power provided by a combination with time-of-flight mass spectrometric detection.
© 2003 Elsevier Science B.V. All rights reserved.

Keywords: Reviews; Multidimensional gas chromatography; Orthogonal separation; Modulation; Gas chromatography, comprehensive two-dimensional

Contents

1. Introduction 70
2. Principle and advantages of GC×GC 71
   2.1. Principle of GC×GC 71
   2.2. Orthogonality and GC column selection 72
      2.2.1. Column dimensions 74
      2.2.2. Gas velocities and temperature programming 75
   2.3. Modulation 75
      2.3.1. Modulation time–wrap-around 77
   2.4. Detectors in GC×GC 77
   2.5. Analytical performance data 78
      2.5.1. Retention time 78
      2.5.2. Quantification 79
      2.5.3. Analyte detectability 80
   2.6. Data processing 81
      2.6.1. Peak integration 81
      2.6.2. Processing of GC×GC–TOF MS data 82

*Corresponding author. Tel.: +31-20-444-7525; fax: +31-20-444-7543.
E-mail address: dalluge@chem.vu.nl (J. Dallüge).

0021-9673/03/$ – see front matter © 2003 Elsevier Science B.V. All rights reserved.
doi:10.1016/S0021-9673(03)00242-5

2.6.2.1. Target analysis 82
2.6.2.2. Nontarget analysis 83
2.6.2.3. Group-type analysis 85
3. Applications 85
3.1. Petrochemical samples: GC×GC–FID 85
3.2. Petrochemical samples: GC×GC–TOF MS 89
3.3. Surface water contaminants and pesticides in food extracts: GC×GC–TOF MS 90
3.3.1. Food extracts 90
3.3.2. Surface water 93
3.4. Fatty acids: GC×GC–FID 93
3.5. Steroids in microalgae: GC×GC–TOF MS 95
3.6. Fly ash: GC×GC–TOF MS 97
3.7. Separation of CBs: GC×GC–μECD 97
3.8. Air analysis: GC×GC–FID 101
3.9. PAHs in sediment: GC×GC–TOF MS 101
3.10. Garlic powder: GC×GC–FID 103
4. Conclusions 104
Acknowledgements 106
References 106

1. Introduction

In recent years, the (trace-level) analysis of complex mixtures such as petrochemical samples or cigarette smoke, food containing a variety of flavours and/or fragrances, and sediments, oils or biota contaminated with polyhalogenated biphenyls or other organic micropollutants, has rapidly gained increasing importance. Conventional gas chromatography (GC) using modern capillary columns offers high peak capacities. However, it fails to separate all the individual constituents (from the matrices) of such complex samples as mentioned above. Therefore, sample preparation by, e.g. multistep solid-phase extraction or size-exclusion chromatography, liquid chromatography (LC) or coupled-column techniques (heart-cut GC [1,2], LC–GC) are frequently used to characterise (often only a part of) the sample, at the expense of very long analysis times and complex instrumentation.

With the introduction of comprehensive two-dimensional gas chromatography (GC×GC) some 10 years ago, a technique has become available which is especially suited for the separation and identification of analytes in complex samples [3–10]. Today, close to one hundred papers are available which discuss the theoretical aspects, the instrumentation and the application of this highly promising separation technique. Impressive results have been obtained in terms of separation efficiency and, also, compound classification based on the presence of ordered structures in the GC×GC chromatograms of (classes of) structurally related compounds. Next to the substantial increase in separation power and speed of analysis compared to the conventional coupled techniques, comprehensive two-dimensional systems provide two complete sets of retention data for all constituents of a sample—which yields an additional tool for their identification.

However, while the technical progress is fairly well documented, and the general strategies to be used to develop methods for GC×GC separations are clear, there is still quite some hesitation for newcomers to enter the field. To our opinion, this is at least to some degree due to a perceived limitation of the application range. In most early and also many subsequent studies, the analysis of petrochemical products was used as an example [11–14]. This is not really surprising because such samples combine several interesting features. They contain a limited number of well-known classes of compounds such as acyclic alkanes (paraffins), cyclic alkanes (naphthenes), and mono-, di- and triaromatics, which, at the same time, each comprise a very large number—possibly on the order of tens of thousands—of individual homologues and isomers.

The analysis usually aims at group-type profiling and, in most cases, detection is straightforward and can be performed by means of a, sufficiently fast, flame-ionisation detection (FID). The emphasis on this—also economically and technologically highly important—type of applications has fed the, false, impression that GC×GC, although generating an impressive separation efficiency, is not as important for other GC-based analyses as is sometimes claimed.

In order to dispel the above impression and demonstrate the versatility and wide-ranging applicability of comprehensive two-dimensional GC as an analytical tool, a number of mutually widely differing examples of GC×GC analyses of real-life samples is discussed in this paper. In each instance, essential information concerning the analytical strategy and separation will be provided, with special emphasis on the added value of the use of GC×GC instead of 1D-GC. As regards detection, the benefits and the drawbacks of the use of time-of-flight mass spectrometric (TOF MS) detection will be highlighted. All examples are taken from published or on-going work in which the present authors participate(d). In the former case, additional information not available in the original publication has sometimes been added. For the convenience of the reader not yet familiar with the underlying principles and instrumentation of GC×GC, a succinct discussion of these topics—and of outstanding problem areas—is included in the review.

2. Principle and advantages of GC×GC

2.1. Principle of GC×GC

In the previous section, it was briefly indicated that the performance of conventional—i.e. one-dimensional (1D)-GC can be distinctly improved by using, instead, a two-dimensional (2D) GC system. Over the years, 2D-GC or GC–GC has been studied in much detail, and large numbers of successful applications of this so-called multidimensional GC have been reported [1,2]. However, one should keep in mind that in essentially all cases, the separations were of a heart-cutting nature. That is, only a single, or a few small fraction(s) of the first-dimension eluate containing the target analytes was/were transferred to the second column for further separation. If the column-to-column interfacing is properly designed, and the second column is sufficiently different from the first one, such heart-cutting can provide substantially enhanced resolution for the target regions: it is an excellent solution if no information regarding the whole sample is required. However, when this is not the case because of either the complexity of the sample type or the emphasis on unknowns rather than target analytes—a comprehensive approach is required. For the present case, this means that GC–GC is replaced by GC×GC, which is a truly comprehensive technique because now, rather than a few selected fractions, the entire sample is separated on two different columns, and no information gained during the first separation is lost during the second one. This is often expressed by saying that, instead of the $(n1 + n2)$ outcome of a heart-cut operation, the comprehensive technique provides the much more beneficial $(n1 \times n2)$ result—where $n1$ and $n2$ are the peak capacity of the first and second column, respectively.

In GC×GC, two GC separations based on fundamentally different separation mechanisms are applied to the entire sample in order to create so-called orthogonal separation conditions [15]. The schematic of a GC×GC system is shown in Fig. 1. Almost invariably, the sample is first separated on a high-resolution capillary GC column—typically a 15–30 m×0.25–0.32 mm I.D., d_f 0.1–1 μm column, containing a nonpolar stationary phase, and using

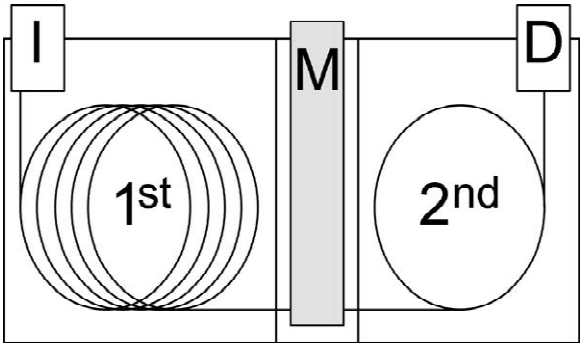

Fig. 1. Schematic of a GC×GC system. I, injector; M, modulator; D, detector; 1st, GC oven with first-dimension column; 2nd, (separate) GC oven with second-dimension column.

temperature programming with a heating rate of no more than 1–5 °C/min. An interfacing device designated as modulator is used to separate the first-column eluate into a very large number of adjacent small fractions. To maintain the first-column separation, these fractions should be no larger than one quarter of the peak width, or σ, in that dimension [16,17]. Each individual fraction is refocused and, subsequently, injected into the second GC column, which is much shorter and narrower than the first column—typical dimensions are 1–2 m×0.1 mm I.D.×d_f 0.1 μm. The second-column separation generally is of a polar or shape-selective nature and, therefore, indeed effects the required orthogonal separation conditions. The separation in this column is extremely fast and takes only 1–10 s as against 45–120 min for the first-dimension separation. Consequently, it is performed under essentially isothermal conditions. In some systems, the second column is housed in a separate oven to allow more flexible and independent temperature programming, while other GC×GC systems only use one oven and thus have identical temperature programming conditions for both columns.

The fast separation in the second dimension results in very narrow peaks with widths of, typically, 100–600 ms at the baseline [18–20]. These narrow peaks require fast detectors with a small volume and short rise time in order to reconstruct the second-dimension chromatograms properly.

The outcome of a GC×GC run (Fig. 2, step 1) is a large series of high-speed second-dimension chromatograms, which are usually stacked side by side ('transformation' in Fig. 2) to form a two-dimensional chromatogram with one dimension representing the retention time on the first column and the other, the retention time on the second column. This transformation (Fig. 2, step 2) into a 2D-matrix array is often performed by laboratory-written software. Visualisation (Fig. 2, step 3) is usually done by displaying the peaks in the 2D plane by means of colours, shading or contour lines to indicate the signal intensity. One should realise that colours or shades of grey have some limitations when used to indicate a wide range of signal intensities, and it is often necessary to use different contrast settings to visualise both major and minor peaks. Occasionally, three-dimensional plots are used.

In the literature, there is general agreement regarding the main advantages of GC×GC over conventional 1D-GC, and also GC–GC [3,4,7,8]. Most strikingly, the peak capacity is much higher, which yields a distinctly improved separation of the analytes in a sample from each other but also, as will be shown below, from interfering matrix constituents. Secondly, due to the refocusing process in the modulator, and also the improved analyte separation, detectability is improved. Thirdly, if proper orthogonal conditions are used, chemically related compounds show up as ordered structures, which greatly facilitates group-type analysis and the provisional classification of unknowns. In the next sections, the main aspects of interest introduced in the previous paragraphs will be discussed in some detail. These include orthogonality and GC column selection, modulation and detection, and analytical performance data.

By way of introduction it should be mentioned that the configuration and optimisation of a GC×GC system requires a different and more complex approach than that used for conventional 1D-GC. For example, temperature and carrier gas flow will influence the separations in both dimensions differently, but not independently. Furthermore, additional parameters such as modulation frequency and modulator temperature have to be optimised. A number of papers deal with this topic [21–23]. Fortunately for a newcomer to the field, many applications for different classes of analytes and samples reported in the literature use more or less similar conditions that can be used as a starting point for further optimisation.

2.2. Orthogonality and GC column selection

For orthogonal separation conditions to be created in a GC×GC system, it is necessary to use columns that provide independent separation mechanisms in the first and second dimensions. Here, one should consider that every separation in GC is based on two parameters, viz. (i) the volatility of the analytes and (ii) their interaction with the stationary phase by means of hydrogen bonding, π–π interaction, steric effects, etc. (expressed in terms of activity coefficients) [24]. In addition, one should consider that—while in a truly nonpolar column volatility is the

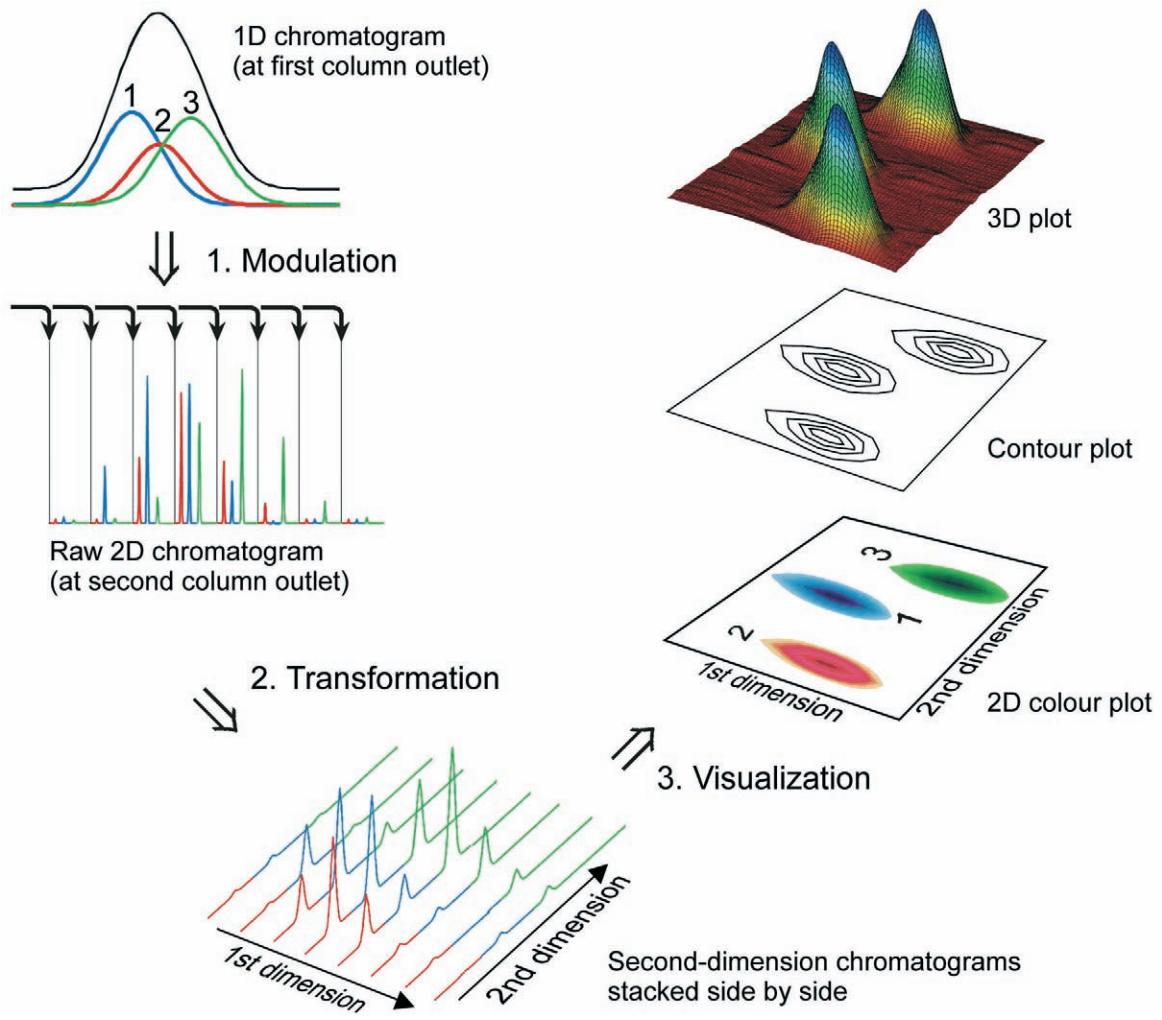

Fig. 2. Generation and visualisation of a GC×GC chromatogram.

only parameter of interest and, consequently, a boiling-point separation is obtained—with all other columns, separation will be governed by the specific interaction(s) of the selected 'polar' column but, also, by volatility. In order, therefore, to achieve orthogonality, the first-dimension column has to be nonpolar. Each individual small fraction eluting from that column will then contain analytes with closely similar volatilities. The subsequent second-dimension separation with its run time of only a few seconds is so fast that it is carried out under essentially isothermal conditions. In other words, for analytes with equal volatility—i.e. the analytes in each individual fraction—there is no boiling-point contribution in the second dimension, and only the specific interaction with the stationary phase governs the retention. That is, the separation is indeed orthogonal.

Stationary phases typically used in first-dimension columns are 100% dimethylpolysiloxane or 5% phenylene–95% dimethylpolysiloxane. In practice, the selection of the first column is also influenced by the availability of an optimised 1D-GC method or retention-index (RI) database for a particular column. In such a situation, the analyst will often be tempted to use such a more polar column. Typical

stationary phases for use in the second dimension are 35–50% phenylene–65–50% dimethylpolysiloxane, polyethyleneglycol (Carbowax), carborane (HT-8) and cyanopropyl–phenyl-dimethylpolysiloxane.

It will be clear that the rewarding result obtained in a nonpolar×polar separation can, in principle, not be achieved by a polar×nonpolar, or a polar×polar, combination. In both instances, the outcome of the first separation will depend on a mix of volatility and polarity effects. Each eluting fraction will therefore contain analytes that differ in volatility, so that volatility also plays a (major) role in the second dimension. As a consequence, the separations in the first and second dimensions are not independent.

Orthogonality is, of course, not a goal in itself. The most important spin-off is that the complete 2D plane of separation can be used and that ordered structures show up in the GC×GC chromatogram [25]. Such structured 2D chromatograms are required to perform group-type identification when analyzing samples that contain structurally related compounds such as homologues or isomers, which is the case in, e.g. petrochemical samples but also in fats and edible oils (fatty acid methyl ester analysis) [26] and mixtures of chlorinated biphenyls (CBs) [27].

One should realise that an orthogonal column combination does not automatically provide structured chromatograms. Two conditions have to be met, (i) the sample has to contain (a large number of) isomers, homologues or congeners, and (ii) the second-dimension column should be chosen dependent on the physicochemical properties of the analytes [25]. One illustrative example was reported by Korytár et al. [27]. They compared several orthogonal column combinations for the separation of planar CBs from other congeners. The best overall separation was obtained on a HP-1×Carbowax combination; however, little or no structure was obtained. Only a HP-1×HT-8 column combination provided structured chromatograms. A somewhat similar conclusion can be drawn from a paper by Haglund et al. [28], who used a polar (liquid crystal phase)× nonpolar (BPX-5) column combination to separate planar CBs from other congeners. Again, the separation of the, limited number of, planar CBs was fully successful, but no structure could be observed in the GC×GC chromatogram.

Nonorthogonal column combinations are also used in the field of enantiomer analysis. The separation of pairs of enantiomers on an enantioselective phase (cyclodextrin) usually requires long run times to obtain sufficient resolution. Therefore, these columns were initially used as the first dimension. Shellie et al. [29] reported successful separations of enantiomeric pairs of monoterpene hydrocarbons and oxygenated monoterpenes with a cyclodextrin×BP-20 (polyethyleneglycol) column combination; however, little structure was obtained. Later, the same group developed an orthogonal system for the same separation using a DB-5×cyclodextrin combination [30]. The separation speed in the second column was increased by using vacuum outlet conditions. Because the latter system provided a first-dimension separation according to volatility and a second-dimension enantioselective separation, more structured plots, featuring the enantiomeric pairs, showed up.

Table 1 lists a selection of frequently used column combinations, both orthogonal and nonorthogonal, and their application area.

2.2.1. Column dimensions

In general a conventional-size column is used in the first dimension, typically 15–30 m×0.25 mm I.D. Selecting the dimensions of this column also depends on the desired separation. In many cases where there already exists a 1D-GC method for the sample under consideration, the first-dimension column will be the column that is conventionally used for the 1D-GC separation.

The separation in the second column has to be completed in a few seconds, and band broadening of the very narrow pulses generated by the modulator should be minimised. Therefore, short narrow-bore columns are commonly used in the second dimension, typically 0.5–2 m×0.1 mm I.D. Recently, the use of a 0.05 mm I.D. column has been reported [34] which provided an ultra-fast second-dimension separation of 1 s and, consequently, a much faster, i.e. 3–4-fold, total analysis.

The use of a conventional column in the first dimension and a gas flow similar to those routinely applied in 1D-GC (as will be explained below) allows the application of virtually all injection techniques. Split, splitless, on-column, large-volume injections (10 μl) using a programmed temperature

Table 1
Examples of column combinations used in GC×GC

Application	Column combination	Orthogonal	References
Essential oils	30 m, 0.25 mm I.D., 0.25 μm BPX5 × 2 m, 0.1 mm I.D., 0.1 μm BP20	Yes	[31]
Enantiomers in essential oils	25 m, 0.25 mm I.D., 0.25 μm 30% β-CD × 0.8 m, 0.1 mm I.D., 0.1 μm BP20	No	[29]
Enantiomers in essential oils	10 m, 0.1 mm I.D., 0.1 μm DB-5 × 1 m, 0.25 mm I.D., EtTBS-β-CD	Yes	[30]
Petroleum	10 m, 0.25 mm I.D., 0.25 μm DB-1 × 0.5 m, 0.1 mm I.D., 0.14 μm OV1701	Yes	[32]
Pesticides in food	15 m, 0.25 mm I.D., 0.25 μm DB-1 × 0.8 m, 0.1 mm I.D., 0.1 μm BPX-50	Yes	[33]
CBs	10 m, 0.15 mm I.D., 0.1 μm LC-50 × 0.25 m, 0.1 mm I.D., 0.1 μm BPX-5	No	[28]
CBs	30 m, 0.25 mm I.D., 0.25 μm HP-1 × 1 m, 0.1 mm I.D., 0.1 μm HT-8	Yes	[27]

vaporiser (PTV) [33] and solid-phase microextraction (SPME) [35,36] have all been utilised.

2.2.2. Gas velocities and temperature programming

Since the two columns are connected in series, their carrier gas velocities cannot be selected independently and a compromise is generally chosen that provides acceptable separation in both dimensions. The linear velocity in the first dimension is usually low (typically 30 cm/s), but still in the optimum range for this column; much lower values will cause a drastic loss of the separation efficiency. At the same time, the linear velocities in the (narrow-bore) second dimension are typically much higher than 100 cm/s, i.e. they are far above the optimum value. This can, however, be tolerated because of the flat slope of the van Deemter curve for these narrow-bore columns.

In order to enable at least three or four modulations to be made over each first-dimension peak, the temperature programming rates in GC×GC are generally lower than in 1D-GC, i.e. only 0.5–5 °C/min. In GC×GC systems with independent temperature control of the two columns, the temperature of the second column is usually programmed at the same rate, but at up to 20–30 °C, usually higher, temperatures. This enables a fine-tuning of the retention in the second dimension as will be discussed in Section 2.3.

2.3. Modulation

The modulator can be considered the 'heart' of a GC×GC system and, consequently, in the early years much effort was devoted to the development of a robust and user-friendly modulator with a wide application range. Independent of its design, a modulator must serve three functions: (i) to continuously accumulate or trap small adjacent fractions of the effluent from the first column whilst the first-dimension separation proceeds; (ii) to refocus the trapped fractions either in time or in space; (iii) to inject the refocused fractions as narrow pulses into the second-dimension column. In practice, the modulator works with a constant frequency of, typically, 0.1–1.0 Hz. In other words, seconds-wide fractions of the effluent of the first column are accumulated and refocused in the modulator and subsequently injected into the second column. Usually, the separation in the second-dimension system is finished before the injection of the next fraction (for wrap-around, the exception, see below). In the present section, a short overview of the most common modulators is presented (see also Table 2 below).

The first modulators were dual-stage thermal desorption modulators which were difficult to manufacture and were not very robust [11,37]. The first commercially available modulator was the so-called Sweeper [38–40]. A thick-film capillary was used to retain and accumulate the analytes at the end of the

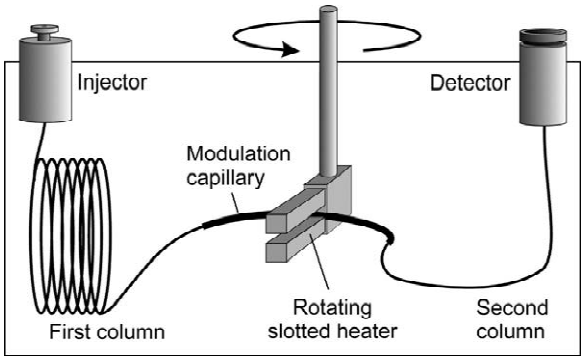

Fig. 3. Schematic of a GC×GC system equipped with a Sweeper.

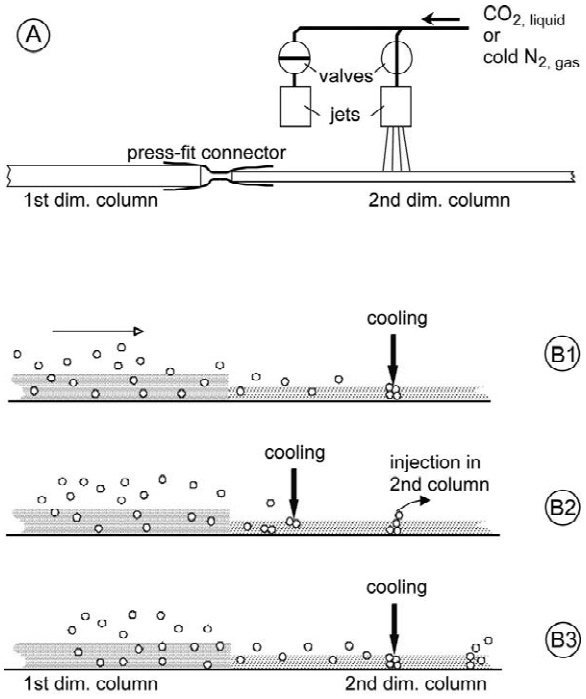

Fig. 4. (A) Schematic of a two-jet cryogenic modulator; (B1–3) principle of cryogenic modulation. (B1) The modulator (right-hand jet) retains part of a peak eluting from the first column. (B2) The right-hand jet is switched off, the cold spot heats up very quickly and the analytes are released and launched for separation in the second column. Meanwhile, the left-hand jet is switched on to prevent material eluting from the first column to interfere with the focused fraction. (B3) The right-hand jet is switched on again and the next modulation cycle is started.

first column by 'phase-ratio focusing', and reinjection was achieved by heating the capillary with a moving slotted heater. The typical set-up is shown in Fig. 3. Next to the complicated nature of the installation and the fact that the slotted heater moves uncomfortably close to the modulator capillary, the major disadvantage of the Sweeper was its limited application range (maximum elution temperature, 230 °C). On the other hand, one should realise that in some 30% of the GC×GC research papers published to date, a Sweeper was used as modulator.

Next, Marriott developed a moving modulator which uses expanding liquid carbon dioxide for cryogenic trapping and focusing of the analytes in the first centimetres of the second column (longitudinally modulating cryogenic system, LMCS) [20,39,41–45]. Reinjection is achieved by moving the modulator (longitudinally) away and heating the spot that holds the focused fraction by means of the oven air. The application range is much wider, but volatile analytes are not sufficiently retained.

More recently, several different versions of cryogenic jet systems were introduced [19,46–48]. Similar to the LMCS they use cryogenic means (expanding liquid CO_2, expanding gaseous CO_2 or nitrogen gas cooled to −180 °C) to retain the analytes. There are, however, no moving parts and the jet systems are therefore more robust. A schematic of the general set-up of such a modulator is shown in Fig. 4. Reinjection is achieved either by switching the modulator off—with the oven air then heating the capillary and, consequently, the part that holds the focused fraction—or by using a pulse of hot air [46,47]. Jet modulators that use cooled nitrogen gas have the lowest trapping temperature and, thus, the widest application range at the low boiling end of the sample.

Another type of modulator uses valves for modulation. Diaphragm valve modulators achieve 're-focusing' by injecting only a small (and, thus narrow) fraction of the eluate from the first into the second column but, because they transfer less than 2% of the eluate, are not suited for trace analysis [49,50]. Valve-based modulators using differential flow modulation transfer about 80% of the eluate of the first into the second column [51]. However, they require a high gas flow-rate in the second dimension to achieve refocusing—in this case, in time, not in

space. Both valve-type modulators are restricted to relatively low temperatures (maximum, 175 °C) which seriously limits their application range.

Table 2 gives an overview over the most common types of modulators, their application range (expressed in boiling-point range of the analytes), reported peak widths and robustness. Other laboratory-made modulator designs are described in [52–56].

2.3.1. Modulation time–wrap-around

In GC×GC, the separation achieved in the first dimension should be preserved during modulation and separation in the second dimension. This means that a peak eluting from the first column should be modulated at least four times, or, in other words, the modulation time should be about 1σ of a first-dimension peak [16,17]. The efficiency of a chromatographic separation is adversely affected and the ordered structure is lost when peaks from different modulation cycles coelute. Therefore, the experimental conditions are usually adjusted such that the modulation time is longer than the retention times of the compounds most strongly retained in the second dimension. Otherwise, analytes will not elute in their own modulation cycle, and cause so-called wrap-around. This effect is illustrated in Fig. 5, which shows the separation of a petrochemical sample using two different second-dimension oven temperatures while all other parameters were kept the same. In Fig. 5A, phenanthrene and anthracene have second-dimension retention times of about 10 s and—when using an 8 s modulation time—elute not in their own, but in the next modulation cycle; that is, they coelute with the monoaromatics of the next modulation. When using a higher temperature for the second-dimension column, the retention time in the column is decreased and the two compounds elute in their own modulation cycle (Fig. 5B). Clearly, the independent temperature control of the second column allows an easy fine-tuning of the GC×GC system.

In principle, wrap-around should always be avoided. However, in actual practice it can be accepted if the compounds showing wrap-around do not coelute with analytes from the next modulation. Illustrative examples are shown in Figs. 17 and 22 of (Sections 3.4 and 3.7, respectively). In both cases, the original plot (shown in the insert) shows wrap-around; however, there is no disturbing coelution and the structure is already visible. The large 2D plots shown in these figures were obtained by combining two or more plots.

2.4. Detectors in GC×GC

The very fast separation in the second-dimension column results in peaks with widths of, typically, 100–600 ms at the baseline [18–21]. The actual peak width depends on the type of modulator used, but also on the gas flow and the dimensions of the second-dimension column and, since this separation

Table 2
Summary of properties of the most relevant GC×GC modulators

Type	Focusing effect			Band width of injection pulse (ms)	Application range (b.p., °C)	Robustness	References
	Phase ratio	Cryo	Valve				
Dual-stage heated	Yes			16–20		− − −	[11,37]
Sweeper	Yes			60	125–450	−	[38–40]
LMCS		CO_2		20–50	125–(550)	+	[20,43–45]
Four-jet cryo		N_2		<10	30–(550)	+ + +	[46]
Two-jet cryo		$CO_{2,\ liquid}$		<10	100–550	+ +	[19]
Single-jet, dual stage cryo		$CO_{2,\ gas}/N_2$		<10	100–550	+ + +	[47]
Single-jet, single stage cryo		$CO_{2,\ liquid}$		<10	100–550	+ +	[48]
Diaphragm valve			Yes	14	0–300	+	[49]
Differential flow			Yes	50	0–300	+	[51]

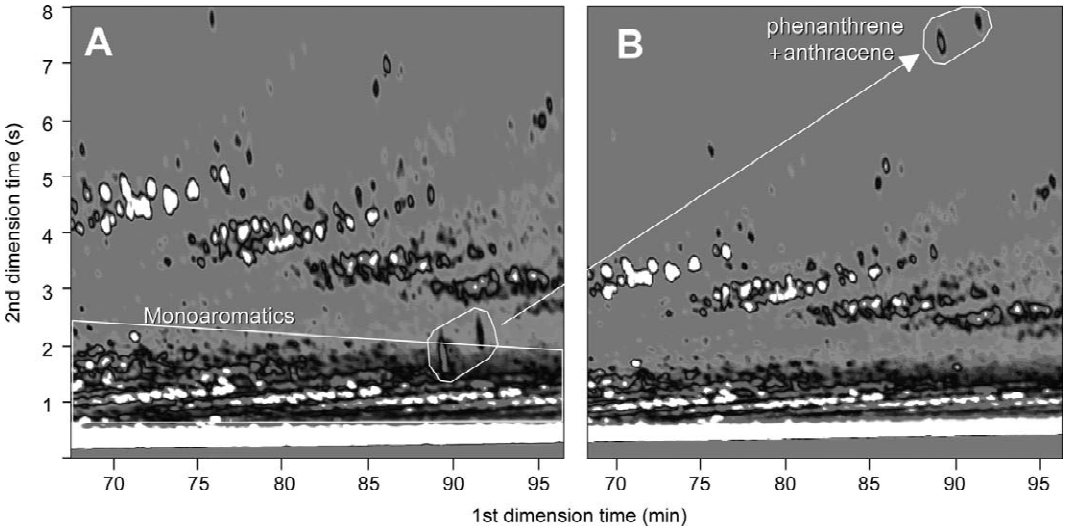

Fig. 5. Part of GC×GC separation of a petrochemical sample illustrating wrap-around. (A) Phenanthrene and anthracene show wrap-around. (B) When using a 20 °C higher temperature in the second dimension, they elute during their own modulation cycle.

is isothermal, on the retention time in that dimension [21]. The narrow peaks require fast detectors with a small internal volume and a short detector rise time and a high data acquisition rate to ensure a proper reconstruction of the second-dimension chromatograms. Therefore, until recently detection in GC×GC was limited to the use of a fast FID. Modern FIDs have a negligible internal volume and can acquire data at frequencies of 50–200 Hz [57]. Today, micro electron-caption detectors (μECD) are also being used in GC×GC; however, their internal volumes of 30–150 μl may still cause extra band broadening [27,58]; the data acquisition frequency of a μECD is typically 50 Hz.

The detectors mentioned above permit peak recognition, but provide no structural information. The use of a spectrometric detector, specifically a mass spectrometer (MS), is therefore indispensable to allow the identification of the numerous separated compounds. At present, only a TOF MS (see Scheme 1) can acquire the fifty or more mass spectra per second that are required for the proper reconstruction of GC×GC chromatograms and for quantification. First results on GC×GC–TOF MS for the analysis of petrochemical samples [59], essential oils [31,35], cigarette smoke [60] and the trace-level determination of pesticides in vegetables [33] were recently reported. They demonstrate an excellent compatibility of the separation and detection parts of the system, even though the, actually four-dimensional, data require new software tools for visualisation and processing. As will be discussed in Section 2.6.2, the amount of data generated per run is overwhelming and data handling is, consequently, rapidly becoming the real analytical problem.

2.5. Analytical performance data

It is true that, generally speaking, less attention has been devoted so far to generating analytical performance data than is usual with a new analytical technique. The dedicated attention that, first, had to be paid to solve the many design and construction problems, at least partly explains the lack of information. On the other hand, this lack is not as serious as it is sometimes made out to be, and the next subsections will demonstrate that, whenever they have been measured, the performance data of GC×GC are found to be fully up to expectation.

2.5.1. Retention time

The run-to-run repeatability and the intralaboratory reproducibility of the first- and second-dimension retention times were investigated by Shellie et al.

In contrast to quadrupole and ion-trap MS instruments, which use an electrical or magnetic field to separate ions according to their *m/z* values, ToF MS instruments measure travel times of ions through a field-free region. The ions are generated in the ion source in a similar way as in the other MS instruments and, then, accelerated as discrete packages into the field-free flight tube by using a pulsed electrical field. Flight times – which are proportional to the square root of the *m/z* value of an ion – are in the order of microseconds. Consequently, ToF MS can be operated at very high repetition rates, typically 5–30 kHz; *i.e.* 5000–30,000 raw mass spectra can be generated per second. Fast detector electronics are required to record the difference in arrival times of the ions at the end of the flight tube. A number of the raw mass spectra are accumulated or averaged and, typically, 10–500 spectra/s are stored in the computer system.

In ToF MS, there are today two more or less complementary approaches, with instruments that provide high mass resolution (5–10 ppm) but have only a moderate scan speed (*ca.* 10 Hz), and instruments that feature a high storage speed of, typically, 100–500 spectra/s but usually provide only unit-mass resolution. Today, such high-speed instruments are increasingly being used successfully as the detector of choice for fast and comprehensive GC.

Scheme 1. Principle of ToF MS

[61]. They found that the run-to-run repeatability for 43 compounds in an essential oil was generally better than 50 ms (1.5%, $n=6$) in the second dimension for peaks with a mean peak width of 150 ms (4σ). First-dimension retention times were calculated based on the fitting of a normal-distribution function to the 'pulsed' peak profile of all second-dimension peaks belonging to a single compound. The repeatabilities were generally better than 4 s or 0.2% ($n=6$). The day-to-day reproducibility of the second-dimension retention times was within $\pm 2\sigma$ of the second-dimension peak width and, for most cases, even within $\pm 1\sigma$. Dallüge et al. [21] reported similar results for pesticides in food samples; they achieved a repeatability of 0.11–0.16 s with peak widths of 0.2–0.6 s ($n=5$). De Geus et al. [40] reported standard deviations of the second-dimension retention times of various CBs relative to an internal standard of 0.07 s ($n=8$) with peak widths of 1.3–1.7 s.

In this context, it is of interest to note that several papers report the use of first-dimension retention index (RI) databases for a provisional peak identification or to improve peak identification in GC×GC–TOF MS [60,62]. Western et al. [63] proposed a method of generating an RI database also for the second-dimension separation. Their method involves the repeated injection of reference compounds, typically *n*-alkanes, during a GC×GC run. However, there is as yet no generally accepted model on which the required calculation can be based.

2.5.2. Quantification

As will be explained in the Section 2.6.1, there are various approaches to perform peak integration in GC×GC. In most publications, first the individual second-dimension peaks belonging to one analyte are integrated using conventional integration algorithms and, then, they are summed. Beens et al. [57] compared results obtained in GC×GC–FID and 1D-

Table 3
Comparison of quantification in GC×GC–FID and 1D-GC–FID

Compound	1D-GC[a]	GC×GC[a]	Difference (%)	RSD[b] (%)
Ethylbenzene	4.50	4.46	0.8	0.8
o-Xylene	6.14	6.18	0.7	0.5
n-Nonane	5.88	5.85	0.5	0.6
Isopropylbenzene	9.49	9.45	0.4	0.2
n-Propylbenzene	5.52	5.52	0.1	1.3
sec-Butylbenzene	5.75	5.71	0.7	0.7
p-Cymene	3.85	3.91	1.5	0.5
trans-Decalin	5.80	5.82	0.3	0.3
n-Undecane	3.93	3.94	0.2	1.3
1,2,4,5-Tetramethylbenzene	3.14	3.16	0.6	0.7
1,2,3,4-Tetramethylbenzene	4.90	4.88	0.4	0.6
Naphthalene	1.08	1.04	3.7	2.2

[a] All concentrations in wt.%
[b] Peak areas in GC×GC ($n=14$).

GC–FID. A selection of their data is shown in Table 3. Next to the excellent agreement between the two sets of quantitative data with a difference of less than 1.5% in all but one case, the repeatability of the GC×GC peak area measurements was highly satisfactory, with relative standard deviations of less than 1% for most analytes.

Analytical performance data for GC×GC–FID (linearity and repeatability) were also reported by Frysinger et al. for volatile oxygenates and benzene, toluene, ethylbenzene and xylenes (BTEX) in water using SPME [36], for BTEX and total aromatics in gasoline [64] and oxygenates in gasoline [65]. The results presented by these authors are similar to, but frequently somewhat less good than, those quoted in Table 3. Unfortunately, the authors do not clearly specify the method of calculation used by them. Data on GC×GC–ECD were reported by de Geus et al. [40] who used a series of seven CBs as test compounds. R^2 values of 0.990–0.997 were found over a range of, typically, 2–50 pg injected, and peak area RSDs were 4–6% ($n=8$) at the 10-pg injection level. Quantification of the CBs in a cod liver reference sample gave concentrations within the certification range in five out of seven cases. Quantification based on GC×GC–FID was also successful for fatty acid methyl esters in vegetable oil and fish [26].

Performance data on GC×GC–TOF MS were published by Dallüge et al. [33]. The procedure was applied to the determination of pesticides. Linearity was found to be good with regression coefficients of at least 0.998 (7 data points in duplicate; range, 0.01–3 ng/l of analyte). The repeatability of the peak-area measurements was 5–11% ($n=5$), which can be called satisfactory. More detailed results are given in Section 3.3.

2.5.3. Analyte detectability

It is not really surprising that many studies on analyte detectability in GC×GC emphasise the comparison between this technique and conventional 1D-GC. Such a comparison is not trivial. For example, the limits of detection (LODs) in GC×GC are influenced by the number of modulations across a peak and the retention time in the isothermal second-dimension separation. More importantly for a valid comparison, both the 1D-GC and GC×GC analyses should be carried out under optimum conditions, i.e. the data acquisition should be adjusted to the peak width (typically 10–20 data points across a peak; see e.g. [66] and [21] for FID and TOF MS, respectively). In GC×GC, this is strictly speaking not possible due to the different peak widths in the (isothermal!) second-dimension chromatograms, and the data-acquisition frequency is usually adjusted to the peak width of the narrowest second-dimension peaks. Lee et al. [66] developed a model to predict the sensitivity gain in GC×GC–FID which was in good agreement with experimental data. They achieved a sensitivity enhancement by a factor 4–5 for GC×GC.

For GC×GC–TOF MS, a 2–5-fold increase in sensitivity was found when modulating peaks two or three times [21]. Similar results were recently reported for GC×GC–μECD of CBs: LODs were 3–5-fold lower than in 1D-GC [27]. In this study, the LODs were 10–20 fg of injected mass (also see Section 3.7).

The above results may seem slightly surprising in view of information contained in other studies. These often report substantially higher sensitivity gains for GC×GC compared to 1D-GC, viz. typically 10–70 fold [57,67,68], and quote refocusing in the modulator as the principal cause. However, in these publications signal intensity, instead of signal-to-noise ratio (S/N), enhancement is usually used to express the improvement over 1D-GC, and often the same data acquisition rate is used in 1D-GC and GC×GC.

Actually, in experimental practice, i.e. when analyzing complex samples, analyte detectability is, of course, often limited by chemical noise, i.e. the presence of a high and noisy background generated by coeluting material. Due to the much improved separation provided by GC×GC as compared with 1D-GC—and exemplified by, e.g. Figs. 14, 20 and 25 in Section 3—such interferences are often efficiently separated from the analytes of interest. Consequently, analyte detectability is now frequently enhanced to a degree which is much higher than, and not related to, the formal presentation presented above.

2.6. Data processing

2.6.1. Peak integration

In the literature, several approaches are reported to perform peak quantification in GC×GC. The most common one integrates all individual second-dimension peaks by means of conventional integration algorithms, and, next, sums all peak areas belonging to one 2D peak [27,33,57]. This is done either (i) by using two software programmes, i.e. conventional GC software for peak integration and another programme for subsequent combination of the peaks or (ii) by using laboratory-written software which integrates both steps (e.g. TWEEDEE [57]). An example is given in Section 2.6.2 for the integration of two peaks using extracted-ion chromatograms [21]. The procedure is very similar to the integration of the chromatograms generated by single-channel detectors as performed in, e.g. Refs. [57] and [27] for FID and μECD, respectively. So far, the software cannot (automatically) combine all second-dimension peaks belonging to a single 2D peak and sum their areas. This step is either done manually or by using predefined windows in which all second-dimension peaks are summed (TWEEDEE).

In a second approach, first a so-called base plane is subtracted, and subsequently three-dimensional peak volumes are calculated by means of imaging procedures [69]. There is an on-going discussion on whether this approach can also be applied to the quantification of analytes in complex samples with little or no structured chromatograms. In these samples the base plane correction may fail, which will result in negative peak areas. At present, suitable software is being developed and still has to prove its practicability.

Further, a chemometric approach referred to as the generalised rank annihilation method (GRAM) was presented in the literature, which mathematically resolves (deconvolutes) and quantifies peaks in GC×GC [70–75]. However, this method requires a bilinear structure of the data, which is strictly speaking not the case when using temperature-programmed conditions for the second-dimension column in GC×GC [72]. So far, the technique was applied only to examples in which the analytes have a rather limited boiling-point range. Future work is aimed at the extension of GRAM to GC×GC with temperature programming in both dimensions. Another chemometric approach, trilinear partial least squares (tri-PLS) data analysis, was applied to the quantification of the aromatic and naphthene contents in naphtha [76]. However, this approach also used a constant temperature for the second-dimension column during the entire GC×GC run.

Software tools are required not only for peak integration, but also to handle the (now two-dimensional) calibration peak tables with retention windows of target compounds. Promising software versions use graphical means to visualise the retention windows. They use polygons to define the borders of areas within which all peaks are summed—a useful tool for group-type quantification of, e.g. petrochemical samples. Further, tools are being developed

to indicate the individual peaks found by the integration software.

Apex plots are such a convenient way to improve the visualisation of the peaks which are detected and to reduce the complexity of the plots. These plots typically use a dot or small circle to indicate only the apex of a peak. As was mentioned above, if the peak-finding routine processes the individual second-dimension chromatograms by using algorithms from 1D-GC, all modulated peaks belonging to one 2D peak will be reported separately. An apex plot generated after such data handling is shown in Fig. 6B and should be compared with the original 2D plot of Fig. 6A. Combining the individual second-dimension peaks leads to a much simplified plot (Fig. 6C). Since the peak-finding algorithms can recognise small peaks that are not immediately visible in the contour plots, and since deconvolution algorithms can be applied, the resulting apex plots facilitate the recognition of small and coeluting peaks. The lower parts of the plots of Fig. 6 provide an illustrative example. In summary, apex plots reduce complexity, enhance visibility and simplify the visualisation of group-type separations [21,60]. This is also demonstrated by the examples included in the subsection on group-type analysis in Section 2.6.2.

2.6.2. Processing of GC×GC–TOF MS data

In GC×GC–TOF MS the data-handling situation is even more complicated than was outlined above. The size of the files (100–400 Mbytes) requires powerful computers and sophisticated and intelligent programmes for data handling. Data visualisation now also involves the generation and overlay of extracted-ion chromatograms. Due to the complexity of most samples subjected to analysis by this technique, manual processing generally is not an option and integrated software tools are required for the automated processing of target as well as nontarget analytes [21,60]. Only recently, a dedicated commercial data-processing software package became available. In the present review several different programmes had to be used and, at that time, much manual interaction was still required.

2.6.2.1. Target analysis

Target analysis, i.e. the identification and quantification of analytes of which the retention times and mass spectra are known, can be performed as in 1D-GC–MS. Peaks are identified using retention-time windows and reference mass spectra. Quantification is done as in GC×GC–FID: first the individual second-dimension peaks (usually of the extracted-ion traces) are integrated using algorithms from 1D-GC (upper part of Table 4). The match factors in Table 4 are an indication of how well the acquired mass spectrum matches the reference mass spectrum. Subsequently, the areas of the second-

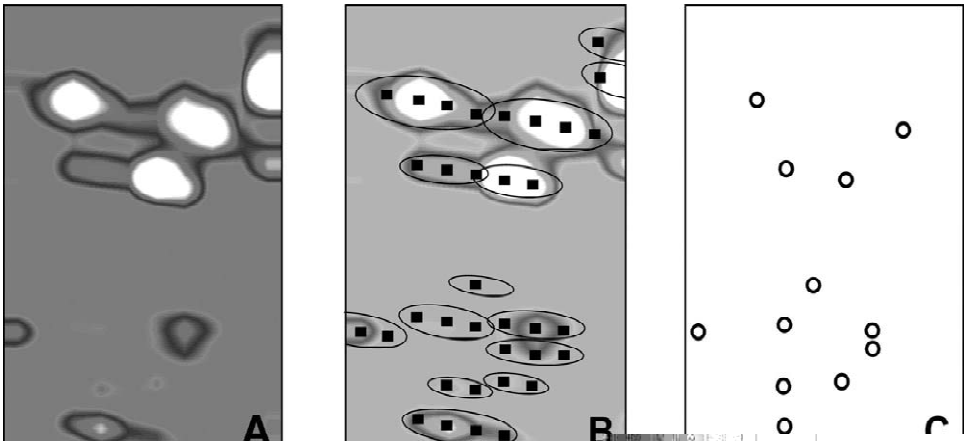

Fig. 6. 2D and apex plots of part of GC×GC–FID chromatogram of a crude oil. (A) 2D plot. (B) 2D plot with apex plot overlaid, showing all individual second-dimension peaks; ellipses indicate the apexes belonging to one 2D peak. (C) Apex plot; individual second-dimension peaks are combined.

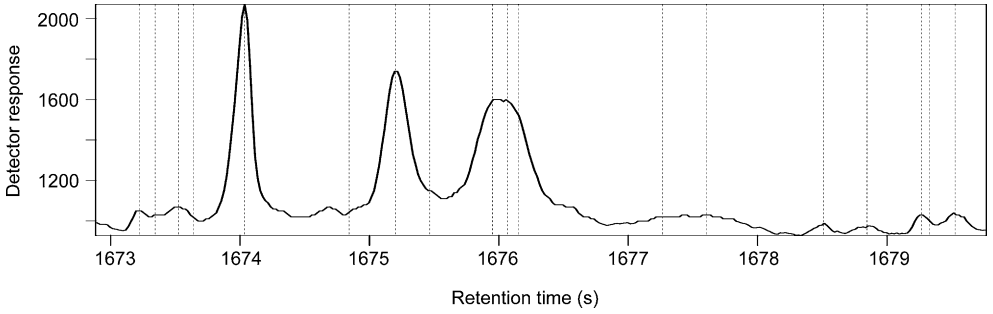

Fig. 8. Part of a (raw) GC×GC–TOF MS chromatogram of a leek extract; vertical lines indicate peaks found by the deconvolution algorithm of the GC–TOF MS software.

shows part of the GC×GC–TOF MS chromatogram of a leek extract. Peaks found by the peak-finding and deconvolution algorithms are indicated by vertical lines. Clearly, these algorithms found many more peaks than are visible in the chromatogram.

The final outcome of the peak finding and deconvolution is a peak table, which contains the library search results, including compound names and mass spectral match factors (similarity, reverse and probability; for further explanation see [21,60]). As an example, Table 5 shows the peak table obtained for the chromatogram of Fig. 8; 19 peaks were found in this 7-s part of the chromatogram. The complete peak table contained more than 2000 peaks. During the postprocessing of this table, library match factors are used to evaluate the reliability of the identification by library search and additional data such as RIs can be used to improve the identification (cf. Section 2.5.1). Peaks with low match factors are either removed or have to be processed manually. To illustrate the only partial success one should add that, in the example of Table

Table 5
Part of peak table with library search results obtained from chromatogram shown in Fig. 8

	t_R (s)	Compound name	Probability	Similarity	Reverse	CAS no.
G	1673.2	Octane, 2,4,6-trimethyl-	813	804	899	62016-37-9
	1673.4	Benzamide, *N*-[[4-[2-(dimethylamino) ...	2680	635	635	00138-56-7
	1673.5	Cyclopentaneundecanoic acid	926	541	693	06053-49-2
	1673.6	Ethyl isoallocholate	2253	550	564	00000-00-0
	1673.8	Benzene, (1-ethyldecyl)-	3733	674	686	02400-00-2
→	1674.0	Tetradecanoic acid	6709	930	933	00544-63-8
	1674.9	8′-Apo-carotenoic acid, 1,2-dihydro ...	3701	595	595	56193-57-8
→	1675.2	Propyzamide	7741	868	868	23950-58-5
	1675.5	Digitoxin	2111	577	608	00071-63-6
	1675.9	Digitoxin	1316	609	612	00071-63-6
	1676.1	Cholesta-8,24-dien-3-ol, 4-methyl-, (3α,4α)-	1267	429	457	07199-92-0
	1676.2	Pyrimethanil	6008	693	700	53112-28-0
	1677.3	Digitoxin	3991	592	677	00071-63-6
	1677.6	Pregnane-7,8,9,11,20-pentaol-18-oic acid, ...	5855	593	604	00000-00-0
	1678.5	Gibbane-1,10-dicarboxylic acid, 2,4a,7-trihydroxy ...	1384	565	593	04747-53-9
	1678.8	Carda-4,20(22)-dienolide, 3-[(6-deoxy-	1368	501	522	20248-01-5
G	1679.3	Nonadecane	908	810	886	00629-92-5
	1679.3	1,1-Dimethylamino-1-butene	3505	643	991	14548-12-0
	1679.5	Perhydroanthracene-2,3,4a,6,7,8a,9a,10a- ...	1372	545	545	00000-00-0

5, only two peaks could be identified (indicated by arrow), while for two other peaks (indicated by G) a group-type identification could be provided.

2.6.2.3. Group-type analysis

In quite a number of applications, there is either not the possibility or not the need to identify all individual peaks. In some cases, fingerprinting aimed at specific classes of compounds is the goal (e.g. petrochemical samples; fats and oils)—in other instances, visualizing a limited number of groups of analytes (e.g. acids, ketones, phthalate esters, aromatic hydrocarbons) in a sample of largely unknown composition is the main aspect of interest. In such situations, a group-type analysis is frequently performed, as was already mentioned in Section 2.6.1 and will be a repeated topic of interest throughout Section 3. Of course, first the contours (polygons) or elution windows of such compound groups have to be drawn. If FID detection is used, this is usually done by injecting standards of suitably selected individual compounds and/or—and this should not be underestimated—on the basis of established knowledge/expertise concerning the nature and composition of the sample type. In actual practice, however, such contours cannot always be recognised very precisely. Typical examples are the crowded higher-boiling part of many samples or cases in which relatively small groups of analytes of interest coelute with other, larger groups of compounds. One such example is the coelution of benzothiophenes and many diaromatics discussed in Fig. 12 below (Section 3.2). Another relevant example, depicted in Fig. 9, shows how MS can—and often should be—used to improve the result. In Fig. 9A, which is the total-ion chromatogram (i.e. a chromatogram comparable with that obtained with FID detection) of a kerosene, the borderlines between the various groups cannot be drawn with much precision: a general indication is all that can be given. If more detailed delineation is required, extracted-ion traces have to be used. In the present example, the m/z values used to generate the plot of Fig. 9B were sufficiently unique to visualise the monoaromatic compounds, i.e. the alkyl-substituted benzenes, while essentially all other sample constituents are 'lost'. Based on this result—and similar ones for the other groups of compounds—it was possible to clearly mark the groups—indicated in Fig. 9A as paraffins, mononaphthenes, dinaphthenes and monoaromatics [59,77].

If there are no sufficiently unique m/z values, apex plots can in some cases be generated by searching a peak table (obtained from nontarget data processing as discussed above) for selected classes of analytes, using compound names and formulae. The corresponding retention times can then be used to generate the plot and draw the required polygons. As an example, Fig. 25 (Section 3.9) shows an apex plot obtained for alkyl-substituted aromatics in a sediment extract. The clusters of the 1–6-ring aromatics are indicated by polygons. In the original GC×GC plot, these groups were not visible due to the presence of many, much larger and partly coeluting peaks.

3. Applications

Table 6 gives an overview of the various application areas in which GC×GC has been applied successfully, classified according to sample type, analytes and detection method. A number of examples from divergent application areas, primarily selected on the basis of our own research work and general experience in these areas, are discussed in some detail in the eleven subsections below. These examples are intended to highlight the potential and versatility of GC×GC, and to illustrate how the various technical aspects of interest discussed in Section 2, are implemented in real-life analyses.

3.1. Petrochemical samples: GC×GC–FID

Petrochemical samples are amongst the most complex samples known to analytical chemists. They contain a very large number of saturated and unsaturated alkanes, cyclic alkanes, aromatics and heteroatom-containing compounds. The total number of compounds in, e.g. a middle distillate has been estimated to exceed one million [12,79]. In many cases, however, the emphasis is on a group-type characterisation only.

The number of compounds in petrochemical samples increases exponentially with the boiling point, and 1D-GC can only fully separate the constituents

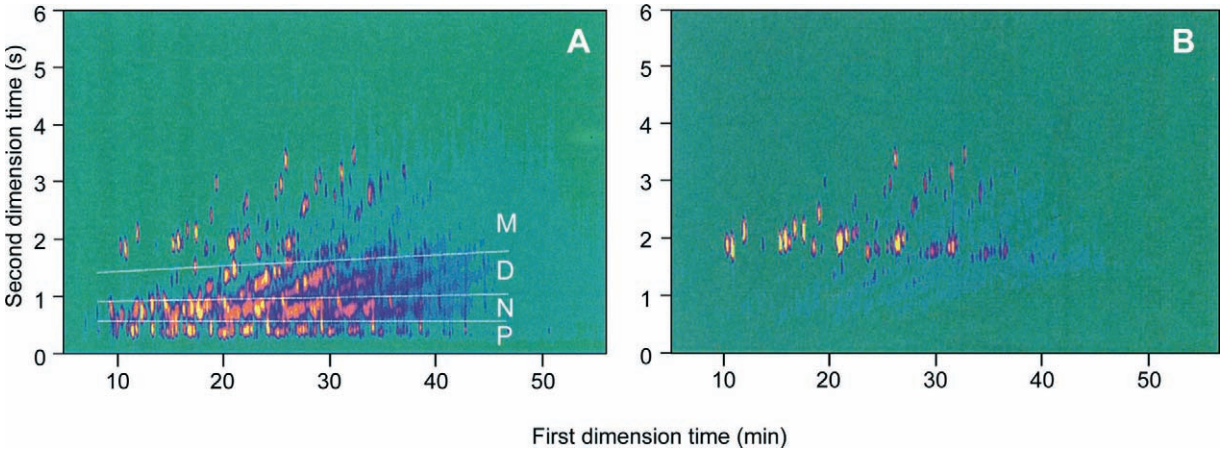

Fig. 9. GC×GC–TOF MS separation of a kerosene. (A) Total-ion chromatogram showing all compounds. To clearly show the group-type separation indicated by horizontal lines (P, paraffins; N, mononaphthenes; D, dinaphthenes; M, monoaromatics), results are required such as are presented in (B) 2D extracted-ion plot constructed by using the sum of the m/z 77, 91 and 105 signals to indicate the monoaromatics [77].

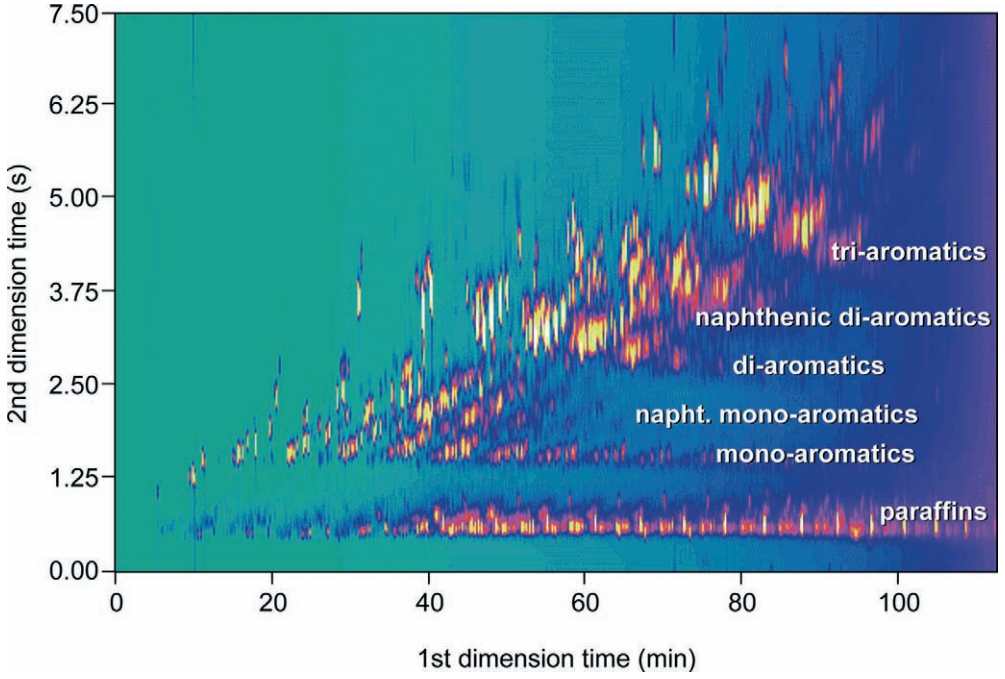

Fig. 10. GC×GC–FID of a light cycle oil using a 25 m×0.25 mm I.D. DB-1×1.5 m, 0.1 mm I.D. OV-1701 column combination and a Sweeper. For further analytical conditions, see [78].

Table 6
Overview of published GC×GC applications

Sample type	Analytes	Target*	Detection method	References
Petrochemical	Group-type characterisation	S	FID	[12–14,32,50,64,65,78–81]
		S	MS	[82]
		S	TOF MS	[58, this paper]
	Biomarkers	A–S	FID	[83]
	Forensic analysis	S	FID	[84,85]
	Target compounds	A–S	FID	[13,64,65]
		A–S	TOF MS	[59]
Essential oils, food extracts	Flavours	S	FID	[35,86–90]
		S	TOF MS	[31,35]
	Enantiomers	A–A	FID	[29,30]
Food (fish) (standards)	PCBs, PCDDs, PCDFs	A–A	ECD	[27]
	PCBs	A–A	FID	[23,28,91]
	Toxaphene	A–A	ECD	[92]
Food (vegetables)	Pesticides	A–S	TOF MS	[33]
Biological oil	Fatty acids	A–A	FID	[26,93]
Algae	Steroids	A–A	TOF MS	[This paper]
Blood plasma	Pesticides	A–S	FID	[94]
Fly ash	Micropollutants	S	TOF MS	[This paper]
Sediment	PAHs	A–S	TOF MS	[54, this paper]
(Surface) water	Volatiles, BTEX	S	FID	[36]
	Microcontaminants	S	FID	[55]
Air/gaseous samples	Volatiles	S	FID	[62,66,95–97]
		S	TOF MS	[75]
Cigarette smoke	General characterisation	S	TOF MS	[60]
Breath	Volatiles	S	FID	[96]
Solvents	Trace-level impurities	A–S	FID	[98]
Kinetic studies			FID	[99,100]

*, Focus primarily on: S, characterisation of entire Sample; A–S, limited number of target analytes in complex Sample; A–A, separation of large number of analytes from each other.

in the very low boiling range, i.e. up to C_9 for straight-run hydrocarbon fractions, and even less far for olefin-containing fractions. Several techniques are used for the characterisation of higher boiling ranges. For instance, the dedicated but very complex column-switching PIONA analyser can perform a group-type analysis for light (gasoline- and naphtha-type) fractions up to a boiling point of 200 °C. Middle distillates (boiling range 150–400 °C) can be characterised by combining normal-phase LC (NPLC) and GC [101]. Here, NPLC provides a group-type separation of aliphatics and mono-, di- and tri(+)-aromatics, with a subsequent boiling-point separation of all groups by GC. Unfortunately, both approaches are complex and difficult to optimise, and require operation by skilled analysts. GC–EI-MS also fails to characterise higher boiling fractions due to the close similarity of the mass spectra of the many structurally related compounds and the frequent absence of molecular ions. Some 10 years ago, an MS instrument was developed that uses so-called Townsend discharge ionisation [102]. This system allows the determination of the boiling-point distribution of various compound types up to C_{40}. Unfortunately, it is not commercially available.

It is therefore not surprising that GC×GC was rapidly applied for the characterisation of petrochemical samples. In one early paper [11], a kerosene was analysed to demonstrate the separation power of the technique. The 2D chromatogram recorded for the orthogonal (nonpolar×polar) separation exhibited over 6000 peaks. In addition, a

highly ordered structure could be observed throughout the 2D plane. It is interesting to mention that this 'eye-opener' required a first-dimension run time of no less than 9 h, and second-dimension cycles of 25 s each—that is, rather unlike what is current practice today.

Fig. 10 shows a typical example of the GC×GC analysis of a light cycle oil using a DB-1×OV-1701 column combination. Paraffins, mono- and diaromatics and their naphthenic derivatives, and triaromatics clearly show up as distinct bands with a further, sometimes highly detailed, subdivision within these bands. 2D plots provide readily interpretable fingerprints of such samples and allow the quantification of specific analytes and the determination of the boiling distribution of many compound classes. This group-type characterisation is much more detailed than that obtained by NPLC–GC. Moreover, all information is obtained in a single run, which dramatically increases the amount of information gained per unit time.

Fig. 11 shows the GC×GC separation of a nonaromatic solvent [14]. Similar to Fig. 10, this chromatogram also shows much structure and many (sub)classes can easily be recognised. Alkanes, mono- and dinaphthenes were separated into roof-tiles which, each, only contain compounds with the same number of carbon atoms. In addition, it was found that alkylcyclopentanes and alkylcyclohexanes are separated from each other. For example, as can be seen in the figure, *n*-octylcyclopentane could be separated from *n*-heptylcyclohexane, a highly unusual and much appreciated result that cannot be obtained by any other separation technique. Furthermore, highly branched alkanes were separated in the second dimension from their less branched isomers, which allowed the determination of the degree of branching of the alkanes. Within one roof-tile (indicated by an ellipse), branching increases from the right-hand (*n*-alkane) to the left-hand (highly branched alkanes) side. The proportion of branched alkanes and the degree of branching provides valuable information to predict fuel properties (expressed as octane and cetane numbers).

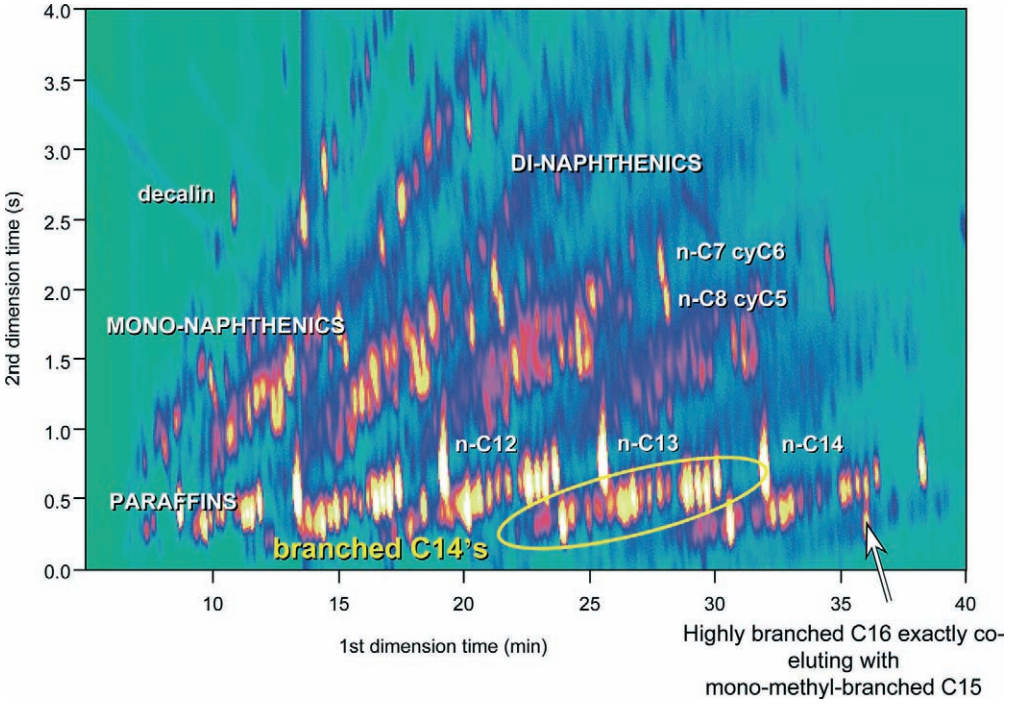

Fig. 11. GC×GC–FID of a nonaromatic hydrocarbon solvent using a 10 m×0.25 mm I.D. CP Sil-2 CB×2.5 m, 0.1 mm I.D. BPX-50 column combination and a Sweeper. For further analytical conditions, see [14].

Beens et al. [57] showed that GC×GC–FID can also be used for quantification. When analyzing single-compound standards, the GC×GC data nicely agreed with those obtained with 1D-GC, and peak area repeatabilities were in the order of 1% ($n=10$). Results for GC×GC group-type analyses of heavy gasoils agreed very well with those obtained with NPLC–GC, but GC×GC provided more detailed results, and in a far shorter time. Since the FID response of hydrocarbons depends to a good approximation only on the mass of carbon in a molecule, quantification of (groups of) analytes can be performed even if no individual standards are available.

3.2. Petrochemical samples: GC×GC–TOF MS

As was argued above, a group-type separation is all that is required in many petrochemical analyses. In some cases, however, emphasis is on a specific group of analytes. One relevant example are sulphur-containing compounds since most of the middle distillates are used as fuel, and combustion of these compounds will contribute to SO_2/SO_3 air pollution. Most sulphur-containing compounds, especially benzothiophenes and dibenzothiophenes, coelute with other groups of hydrocarbons. Consequently, a selective detector has to be used for detection and quantification. With a TOF MS, ion chromatograms can be used to selectively extract such groups of compounds on the basis of their unique masses. TOF MS also enables fast (group-type) identifications during method development.

A middle distillate of a Kuwait oil (174–349 °C) was analysed by GC×GC–TOF MS using a 15 m×0.25 mm I.D.×0.25 μm DB-1 column in the first, and a 0.8 m×0.1 mm I.D.×0.1 μm BPX-50 column in the second dimension. A 1-μl volume of a sample diluted 1:10 in *n*-pentane was injected in the split-mode (1:200). The temperature of both columns was programmed from 70 °C (4 min hold) at 5 °C/min to 300 °C (2 min hold) and an LMCS with a modulation time of 8 s was used. The total-ion chromatogram of Fig. 12A shows the diaromatics part of the separation, which features various classes of compounds such as naphthalenes, biphenyls and benzothiophenes. Due to coelution it is not possible to distinguish the benzothiophenes from the other compounds. This required the use of properly selected extracted-ion chromatograms. In Fig. 12B the molecular ions of the C_1- to C_5-substituted benzothiophenes were used to generate such chromatograms. They clearly show the presence of several compounds belonging to each of these subclasses, as well as the typical roof-tile structure.

As a different example, Fig. 13 shows the use of extracted-ion chromatograms to visualise the elution pattern of alkyldibenzothiophenes and alkylbenzonaphthothiophenes in a catalytically cracked cycle oil, which was analysed under the same conditions as the sample of Fig. 12. The extracted-ion chromatograms allow to distinguish the different groups of the C_1–C_7 alkyldibenzothiophenes. Obviously, there was no complete separation of the C_3- to C_7-substituted species; this would require an improved second-dimension separation on, e.g. longer and/or narrower columns.

The detection of alkyl-substituted dibenzothiophenes and benzonaphthothiophenes is highly important when low-sulphur fuels have to be produced, since these compounds are much more difficult to remove by hydrotreating [103]. Of particular interest is the problem posed by hindered dibenzothiophenes, which have an alkyl substituent adjacent to the sulphur atom, i.e. in the 4- and/or 6-positions. A well-known representative is 4,6-dimethyldibenzothiophene (4,6-DMDBT)

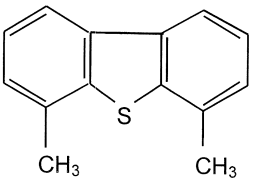

which is highly refractory. The need to use GC×GC to readily identify this, as well as the many related, sulphur-containing compounds is illustrated by the highly characteristic results shown in Fig. 13.

The three nonsubstituted benzonaphthothiophenes showing up in the figure, were also tentatively identified, viz. as benzo[*b*]naphtho-[2,1-d]thiophene, benzo[*b*]naphtho[1,2-d]thiophene and benzo[*b*]-naphtho[2,3-d]thiophene, respectively. However, one should add that with such closely related compounds as are found in each of the subclasses of Fig. 13, the mass spectra are—as a rule—highly similar, and unambiguous identification of the individual

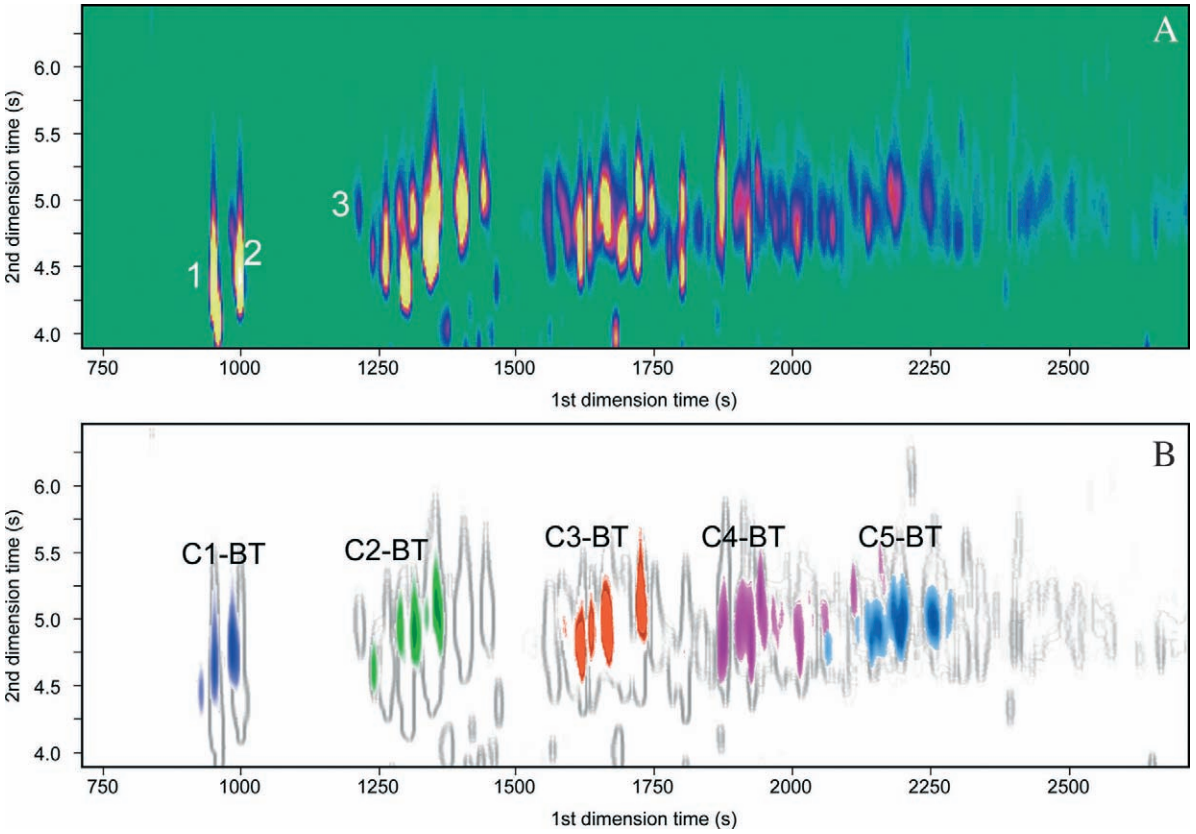

Fig. 12. Detail of GC×GC–TOF MS chromatogram of Kuwait oil using a 15 m×0.25 mm I.D. DB-1×0.8 m, 0.1 mm I.D. BPX-50 column combination and an LMCS. (A) Total-ion chromatogram of diaromatics region, which includes substituted naphthalenes, biphenyls and benzothiophenes. (B) Alkylbenzothiophenes (extracted-ion chromatograms m/z 148, 162, 176, 190, in colour) coeluting with the diaromatics (in grey). 1=2-methylnaphthalene; 2=1-methylnaphthalene; 3=biphenyl; C_1–C_5-BT, substituted benzothiophenes.

analytes (as opposed to that of the groups) requires the availability of pure standards.

3.3. Surface water contaminants and pesticides in food extracts: GC×GC–TOF MS

3.3.1. Food extracts

When analyzing mixtures of compounds with mutually rather different structures, and with a fairly limited number of members in each group, ordered structures will usually be absent. Pesticides, which have to be determined routinely in, e.g. vegetables and fruits, are a good example. The situation typically encountered is that only one or a few pesticides have to be identified and quantified at sub-μg/g concentrations in an often very complex matrix. However, in, e.g. the Netherlands overall about 300 pesticides have to be monitored using multiresidue methods and their number is still increasing due to the introduction of new pesticides. Thousands of samples have to be analysed each year in the Netherlands, and for the EU the number is on the order of 30 000 samples.

Since it is often not possible to sufficiently separate the target analytes from each other and/or the sample matrix by 1D-GC–MS, identification usually relies on a small number of selected m/z values rather than a complete mass spectrum. Consequently, analytes that do not have unique m/z values, e.g. because of strong fragmentation during electron

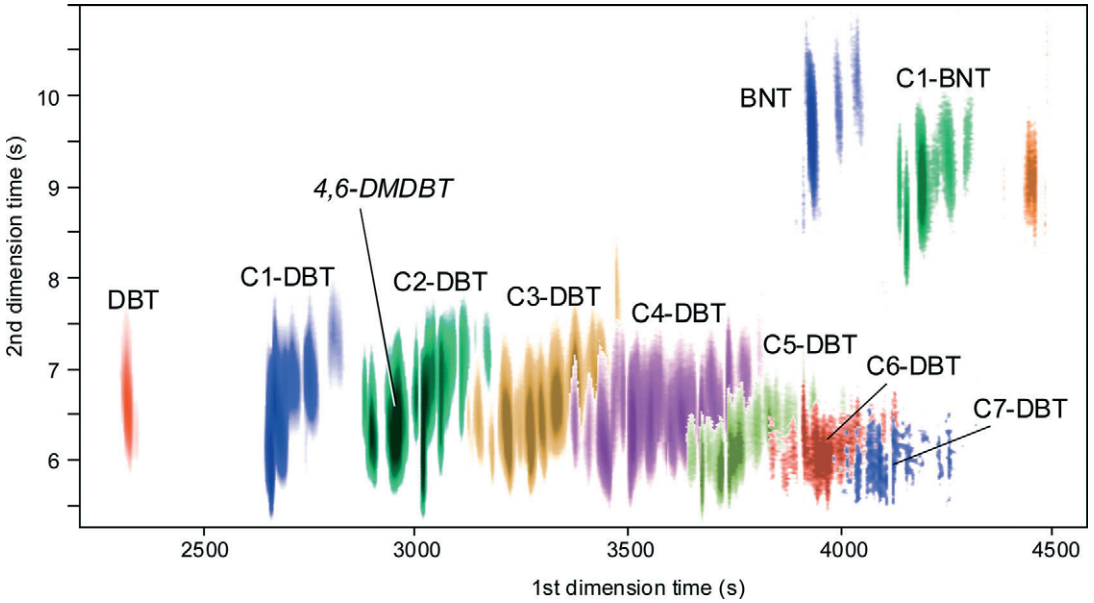

Fig. 13. GC×GC–TOF MS of a light catalytically cracked cycle oil showing the extracted-ion chromatograms (using the molecular ions) of the alkyl-substituted dibenzothiophenes (DBT) and benzonaphthothiophenes (BNT). For conditions, see Fig. 12.

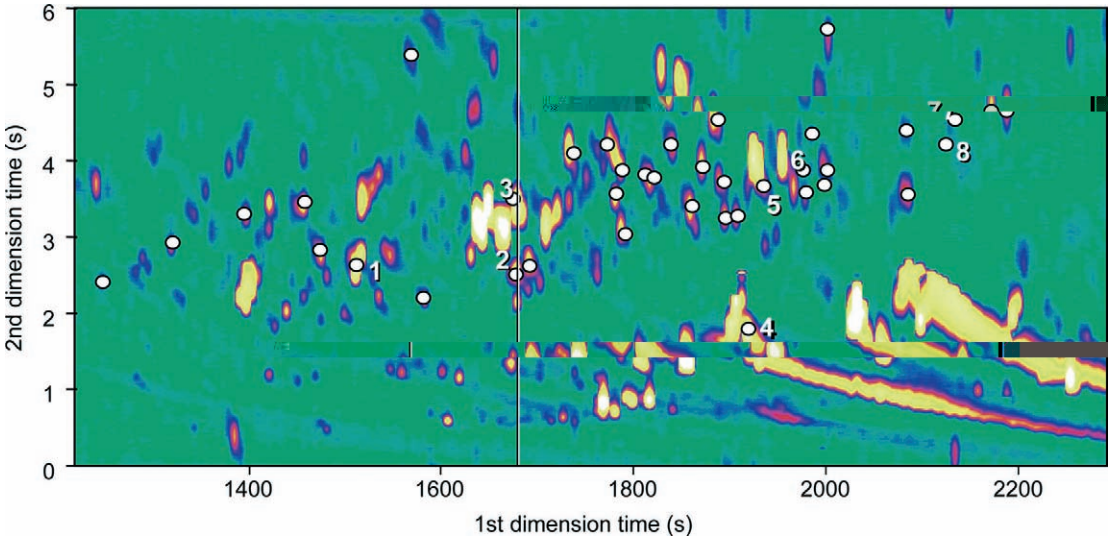

Fig. 14. Detail of GC×GC–TOF MS chromatogram of an extract of leek spiked with a 58 pesticides (each 0.16 ng/μl) using a 15 m×0.25 mm I.D. DB-1×0.8 m, 0.1 mm I.D. BPX-50 column combination and an LMCS. Circles indicate location of apices of pesticide peaks. Peaks: 1=chlorpropham; 2=propyzamide; 3=pyrimethanil; 4=fenpropimorph; 5=bromophos-methyl; 6=chlorfenvinphos; 7=bupirimate; 8=flusilazole. For vertical line at 1678 s, see Fig. 15.

ionisation, are often difficult to detect and require a complex sample preparation to remove interfering matrix compounds.

The potential of GC×GC for the determination of pesticides in foodstuff is demonstrated here with a leek extract. The extract was obtained by blending leek and ethyl acetate at 20 000 rpm, subsequent centrifugation and, next, drying with sodium sulphate. The extract was then spiked with 58 pesticides and an aliquot was subjected to GC×GC–TOF MS with a 15 m×0.25 mm I.D.×0.25 μm DB-1 column in the first and a 0.8 m×0.1 mm I.D.×0.1 μm BPX-50 column in the second dimension.

As will be apparent from Fig. 14, a much improved separation was effected in GC×GC. In addition, mass spectral data could be used to mathematically separate (i.e. deconvolute) partly coeluting peaks, thereby further improving the quality of the mass spectra and increasing the number of peaks that could be properly identified. To quote an example, peaks 1–5 in Fig. 14 partially coeluted with matrix compounds but could nevertheless be identified with high match factors. Part of a second-dimension chromatogram (indicated in Fig. 14 by a vertical line) is displayed in Fig. 15. The deconvolution algorithm recognised the coeluting peaks (such as the pairs M_1+2 and M_2+3) and calculated their pure mass spectra. The final result was most gratifying, as is obvious when comparing the initial (B), deconvoluted (C) and library (D) spectra of peak no. 3, pyrimethanil.

The two very intense and strongly tailing major peaks in the lower right-hand corner of Fig. 14 were found to be due to *n*-hexadecanoic and octadecadienoic acid. Both (nonderivatised) fatty acids show peak tailing in the first dimension. It should be evident by now that, in 1D-GC, these tails will largely obscure all coeluting microcontaminants and, consequently, severely affect the quality of their mass spectra.

It is important to note that all pesticide peaks in Fig. 14 were identified using a nontarget approach as

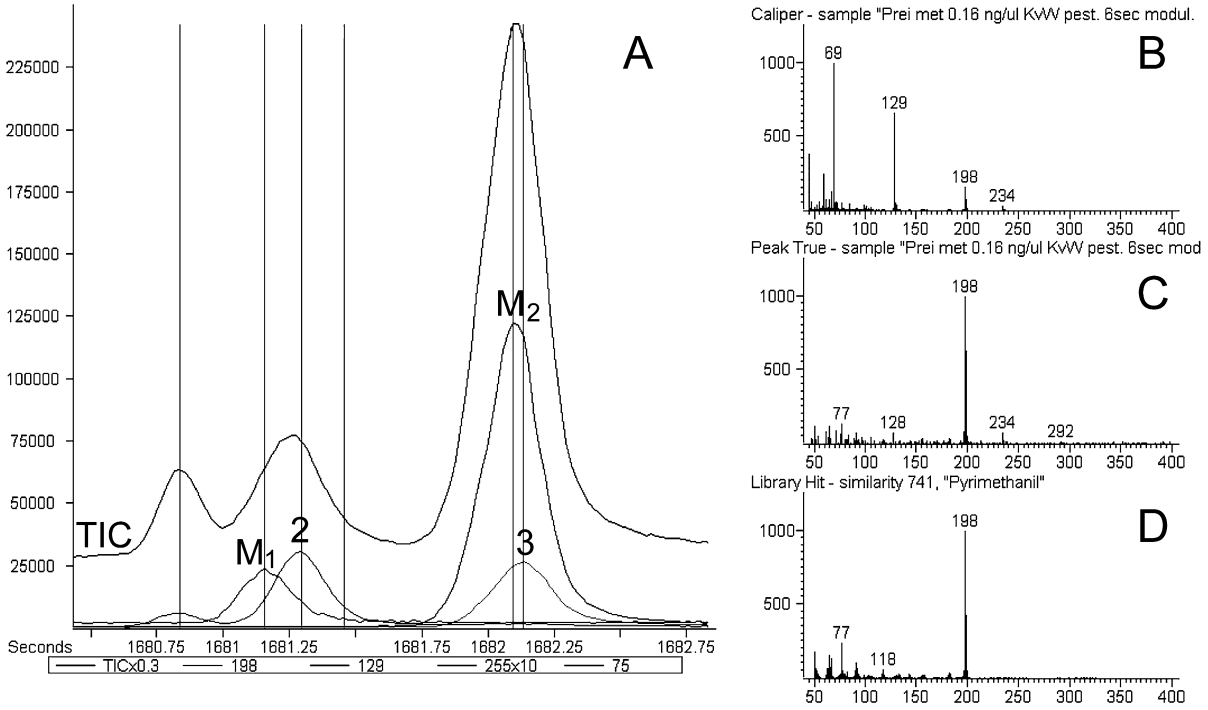

Fig. 15. (A) Part of GC×GC–TOF MS chromatogram of Fig. 14, taken at a first-dimension time of 1678 s, used to illustrate peak deconvolution. Peaks: 2 = propyzamide; 3 = pyrimethanil; M_1 and M_2 = matrix compounds. (B) Mass spectrum at retention time of peak no. 3, (C) the deconvoluted mass spectrum and (D) the library spectrum of pyrimethanil.

explained in Section 2.6.2: the GC–TOF MS software was used to process all peaks found in the chromatogram and the pesticides were searched afterwards in the peak table containing all sample constituents. This demonstrates that GC×GC–TOF MS can also be used for nontarget approach—i.e. to find and identify all suspected contaminants.

As an example of GC×GC–TOF MS-based quantification (cf. Section 2.6.2), Table 7 lists analytical performance data for some selected pesticides. The linearity and repeatability data of the peak area measurements are seen to be fully satisfactory, while the repeatability of the second-dimension retention times is acceptable for the intended application.

3.3.2. Surface water

Surface water is usually considered a not too complicated sample type. However, since the target compounds have to be determined at, typically, ng/l concentrations, GC chromatograms tend to become rather complex because, with such a high level of analyte detectability, many other microconstituents will show up and may well interfere. Consequently, improved separation efficiency is desirable.

Fig. 16 shows the separation of a mixture of microcontaminants that are frequently found in surface water [104]. Analysis was carried out on 30 m, 0.32 mm I.D., 0.25 μm HP-1×1.5 m, 0.1 mm I.D., 0.1 μm BPX-50 column combination, and with a moving cryogenic modulator (see [55]). The mixture contained compounds as divergent as alkyl-, nitro-, and chlorinated benzenes, phenols, anilines, alkyl phosphates and a number of pesticides. Consequently, it is not surprising that, as with the previous example, ordered structure is not a main feature of the 2D chromatogram. The separation conditions, however, appear to have been well-chosen: the peaks of the analyte mixture are seen to be distributed over almost the entire GC×GC plane. In addition, even though there is little structure, also in this case, it is possible to find a relationship between chemical structure and second-dimension retention time. Two examples are indicated in the figure: the nitrobenzenes all elute at second-dimension times of 5–6 s, and chlorinated benzenes much earlier, viz. at 2.7–3.7 s.

3.4. Fatty acids: GC×GC–FID

The analysis of fatty acids is of significant interest because of their important role in human diet, and also for therapeutic reasons. They are also used as biomarkers, e.g. for the characterisation of microalgae. Fatty acids can be classified as saturated, mono- and polyunsaturated (PUFAs) fatty acids. Fats containing PUFAs are liquid at room temperature and are called oils. There is a distinct difference in the composition of vegetable oils and fish oils. The former contain PUFAs with two or three double bonds, and the latter a larger proportion of PUFAs with five or six double bonds, and also a number of fatty acids with an odd number of carbon atoms. PUFAs such as eicosapentaenoic acid and docosahexaenoic acid are known to play a major role in the cardiovascular system, and the central nervous, immune and visual systems.

Fatty acids are usually analysed after conversion into their methyl esters (FAMEs), with subsequent

Table 7
Analytical performance data of selected pesticides

Analyte	^1t_R (s)	^2t_R (s)	Quantification mass (M_r)	LOD[c] (pg)	Correlation coefficient[a]	RSD of peak area (%) [b]	SD (s) of 2nd dimension retention time
Molinate	881	2.4	126	5	0.9994	11	0.11
Trifluralin	1097	1.0	264	7	0.9994	8	0.11
Prometryn	1355	2.9	241	12	0.9978	7	0.16
Metolachlor	1427	2.2	162	5	0.9988	6	0.11
Stirofos	1577	3.2	109	23	0.9981	9	0.16
Butachlor	1601	2.0	160	7	0.9996	5	0.14

[a] Range, 0.01–3 ng/μl; 7 data points in duplicate.
[b] Determined at a level of 100 pg, $n=5$.
[c] Experimentally determined at 10–30 pg level for the highest second-dimension peak, 3×peak-to-peak noise.

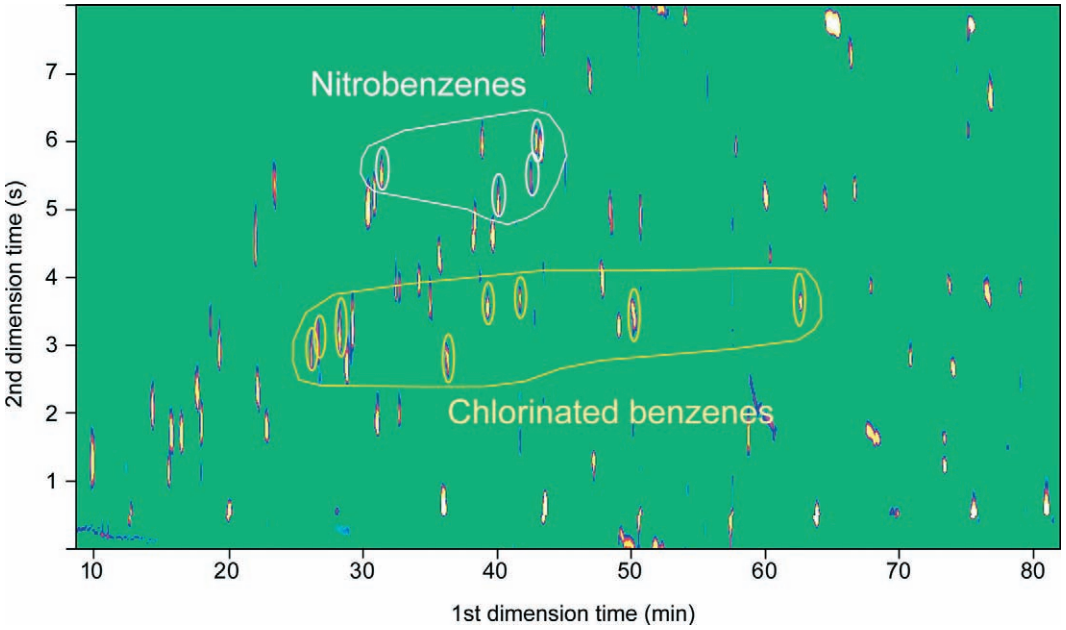

Fig. 16. GC×GC–FID of a mixture of 80 microcontaminants typically found in surface water. The ellipses indicate the positions of: (white) nitrobenzenes and (yellow) chlorinated benzenes. Conditions: for columns, see text; temperature programme, 30 °C (2 min hold), 2 °C/min to 300 °C; laboratory-made cryogenic modulator.

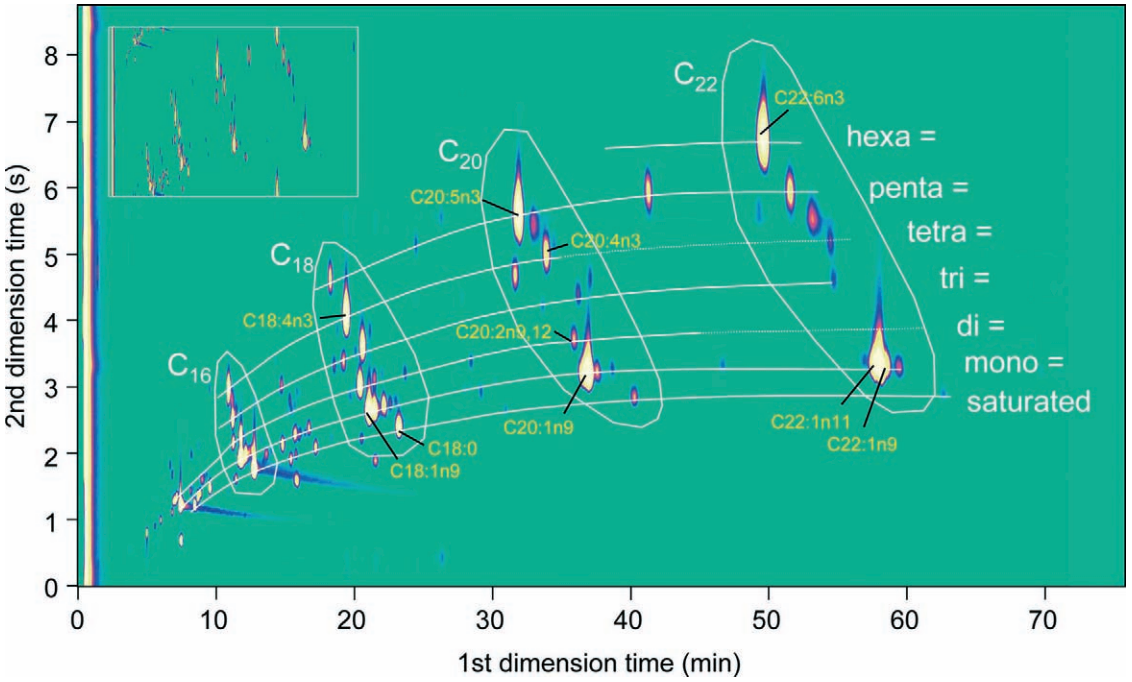

Fig. 17. GC×GC–FID of herring oil sample using a 9 m, 0.2 mm I.D. HP-1×0.3 m, 0.1 mm I.D. CP-Wax-52 column combination and a Sweeper. Lines indicate fatty acids with same number of double bonds, and polygons fatty acids with same number of carbon atoms. The original 2D plot (insert) was modified to avoid wrap-around. For detailed analytical conditions, see [26].

1D-GC (–MS). The large number of compounds with, frequently, closely similar structures complicates such a separation and recently an attempt was made to enhance the overall resolution by using GC×GC as an alternative separation technique. The 2D plot of the GC×GC–FID analysis of fatty acids, as their FAMEs, present in a herring oil sample is shown in Fig. 17. Analysis was performed using a 9 m×0.2 mm I.D.×0.33 μm HP-1 column in the first, and a 0.3 m×0.1 mm I.D.×0.2 μm CP-Wax-52 column in the second dimension [26].

The GC×GC chromatogram clearly shows that the FAMEs are separated into more or less parallel bands according to their number of double bonds, which is seen to range from zero (saturated) to six. Retention in the second dimension distinctly increases with the number of double bonds. As indicated by the polygons in Fig. 17, fatty acids with the same number of carbon atoms elute as clusters. Part of the structural information presented here was not contained in the original study. In other words, the number of carbon atoms and double bonds of an unknown fatty acid can easily be predicted from its position in the GC×GC plane—even with FID detection. In the quoted paper, this was done for an unknown peak which was tentatively identified as C_{20}:1n9, with the provisional identification being confirmed when a standard became available. The potential of GC×GC was also demonstrated by the provisional identification of several fatty acids with an odd number of carbon atoms of which no standards are available: several peaks were identified as C_{19} fatty acid congeners with zero to three double bonds. Finally, quantification, especially of the minor sample constituents, was significantly improved due to the much improved separation. Quantification was performed for a series of vegetable and fish oil samples, with results that could readily be explained on the basis of the origin and/or heat pretreatment of these samples.

3.5. Steroids in microalgae: GC×GC–TOF MS

In microalgae, a large diversity of sterols and steroidal ketones has been found [105]. Some of these compounds are widely distributed, while others are found only in some specific species and are therefore useful as chemotaxonomic markers. Microalgae are major sources of lipids in lacustrine and marine environments and the markers are used to identify the sources of organic matter in sediments. Sterol distributions in microalgae range from the predominance of a single compound to mixtures of ten or more in, e.g. dinoflagellates. Sterols are usually analysed as their trimethylsilylether (TMS) or acetate derivatives by 1D-GC–MS. Sterols and steroidal ketones belong to the class of steroids, which all contain a four-ring cyclopentanoperhydrophenanthrene nucleus. Steroids having a saturated ring system are called steranes (Fig. 18A). Usually, in algae sterols have a hydroxyl group (Fig. 18B), or in the case of steroidal ketones, a keto

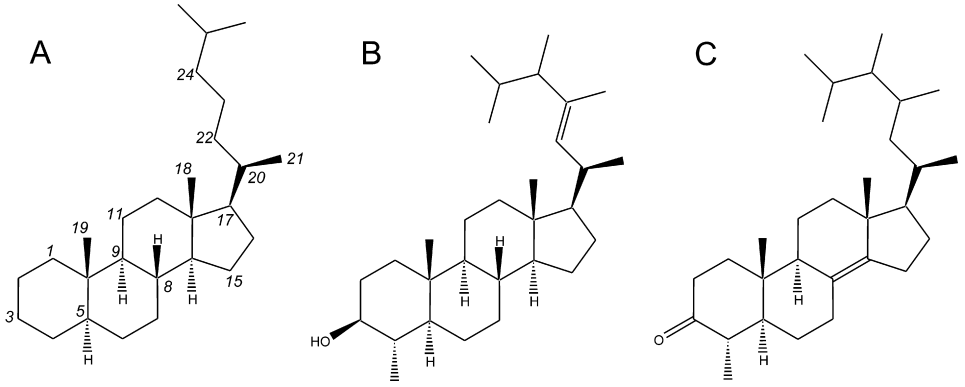

Fig. 18. Structures of steroids (numbering indicated in A). (A) 5α-Cholestane as example of a sterane, i.e. a steroid with no functional group; (B) 4α,23,24-trimethyl-5α-cholest-22E-en-3β-ol (dinosterol) as example of a sterol; (C) 4α,23,24-trimethyl-5α-cholest-8(14)-en-3-one as example of a steroidal ketone.

group in the 3-position (Fig. 18C). Sterols and steroidal ketones typically have 27–30 carbon atoms.

A sample of the dinoflagellate Calciodinellum operosum was extracted with dichloromethane and derivatised with N,O-bis(trimethylsilyl)trifluoracetamide (BSTFA) in pyridine to convert compounds containing free hydroxyl groups into their TMS derivatives. The extract was then analysed by GC×GC–TOF MS, with the use of a 15 m×0.25 mm I.D.×0.25 μm DB-1 column in the first, and a 0.8 m×0.1 mm I.D.×0.1 μm BPX-50 column in the second dimension. A 10-μl volume of the extract was injected using an Optic 2 injector in the solvent-vent mode. The temperature of both columns was programmed from 70 °C (4 min hold) at 20 °C/min to 150 °C and at 2 °C/min to 325 °C (2 min hold). An LMCS modulator was used, and the modulation time was 6 s. Full-scan mass spectra were acquired in the range m/z 35–600. The sterols and steroidal ketones eluted at temperatures of 260–280 °C. Therefore, cryogenic modulation was essential since heated modulators (such as the Sweeper) and valve-based modulators cannot be used at such high temperatures.

Fig. 19 shows part of the GC×GC chromatogram of an extract that was found to contain a number of sterols, steroidal ketones and steranes. To the best of our knowledge, this is the first attempt to apply GC×GC to the analysis of steroids. Related chemical structures are again seen to dominate the positions of the analytes in the GC×GC plane. All steroids (as their TMS derivatives) elute at second-dimension times of about 2 s and have even shorter retention times than most of the steranes. Obviously, the TMS group causes a decrease of the retention in the second dimension. Similar observations are made in Section 3.6, below, where siloxanes have shorter retention times than alkanes. Steroidal ketones were

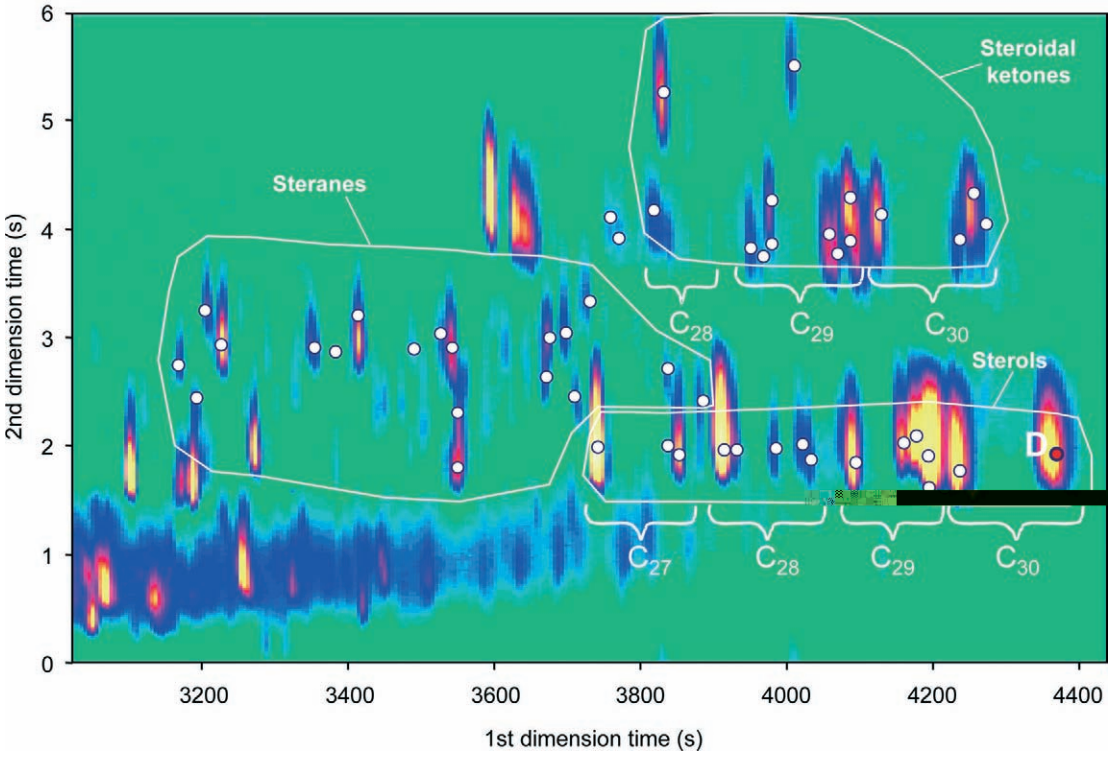

Fig. 19. Detail of GC×GC-TOF MS total-ion chromatogram of an extract of Calciodinellum operosum, after derivatisation with BSFTA. Conditions: 15 m, 0.25 mm I.D. DB-1×0.8 m, 0.1 mm I.D. BPX-50 column combination and an LMCS. Temperature programme: 70 °C (4 min hold), 20 °C/min to 150 °C, 2 °C/min to 325 °C (2 min hold). Peaks: D=dinosterol.

have the highest second-dimension retention times. In other words, and this was confirmed by further study of the results for the other CBs, on each isochlorine dotted line, the number of orthochlorine substituents increases from the top to the bottom end of these lines. Finally, it is interesting to add that the other column combinations tested (HP-1×BPX-50 and HP-1×Supelcowax-10) showed hardly any ordered structure, even though with the latter combination, the overall CB resolution was better (cf. Section 2.2).

In a second example, a mixture containing 90 CBs and the 17 most toxic PCDDs and PCDFs was analysed using the HP-1×HT-8 column combination; the 2D plot is shown in Fig. 22 [27]. The CDD and CDF congeners were separated from each other and also from all but one CB (CB 169 coelutes with a penta-CDD or -CDF). This impressive separation was achieved without any preseparation, which is always required in conventional GC analysis. In this GC×GC–μECD chromatogram, most of the CDDs and CDFs show wrap-around; however, in contrast to what was shown for the petrochemical sample of Fig. 5, the separation of the analytes of interest was not adversely affected. Still, for convenience, the chromatogram of Fig. 22 was modified to show the peaks at their true second-dimension times: the broken line indicates the modulation time of 6.5 s, and the insert shows the original GC×GC chromatogram.

Table 9
LODs of selected CBs in GC×GC–μECD compared with GC–μECD

CB no.	Molecular formula	LOD (fg)[a]	
		GC	GC×GC
44	$C_{12}H_6Cl_4$	60	20
97	$C_{12}H_5Cl_5$	50	10
105	$C_{12}H_5Cl_5$	40	10
118	$C_{12}H_5Cl_5$	40	10
137	$C_{12}H_4Cl_6$	30	10
156	$C_{12}H_4Cl_6$	30	10
180	$C_{12}H_3Cl_7$	40	10
194	$C_{12}H_2Cl_8$	40	10
206	$C_{12}HCl_9$	70	20

[a] Determined at S/N of 3:1.

The LODs of some selected CBs are given in Table 9. For most CBs, LODs of about 10 fg were

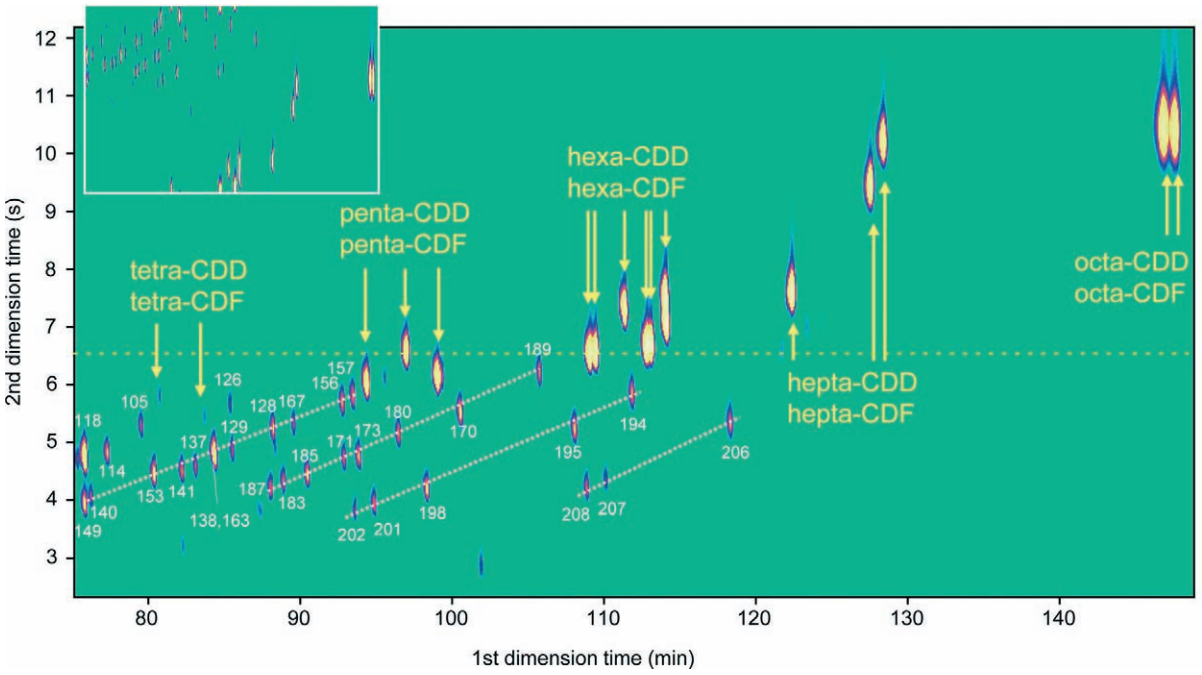

Fig. 22. Part of GC×GC–μECD chromatogram of a mixture of 90 CBs and 17 PCDDs and PCDFs using the same conditions as in Fig. 21.

obtained, which is approx. 3–5-fold better than with GC–μECD. Similar sensitivity improvements were also reported in other studies for other detectors, as was discussed in Section 2.5.3. Relevant data on linearity and repeatability as determined in another study [40], were already discussed in Section 2.5.2.

3.8. Air analysis: GC×GC–FID

Volatile organic compounds (VOCs) play an important role in the atmosphere. They are, for example, precursors for the formation of tropospheric ozone, while halocarbons are known to destroy stratospheric ozone, organic acids contribute to the acidification of precipitation, and other compounds act as greenhouse gases. Typically, VOCs are analysed by GC–FID or GC–MS. However, severe peak overlap in 1D-GC readily causes difficulties in identification and/or inaccuracy in quantification. The issue is further complicated by the low concentrations of some analytes, which are, therefore, easily masked by (larger) coeluting peaks. Lewis et al. [97] demonstrated that GC×GC greatly enhances the separation, and reveals many more compounds in an urban air sample than are usually reported in 1D-GC measurements. As an example, in an 8-min part of a GC×GC chromatogram they found 110–120 compounds, while only 20–30 peaks were visible in the same part of a 1D-GC chromatogram.

During the Mediterranean intensive oxidant study (MINOS) project, in situ measurements of air samples were performed using GC×GC–FID [62]. The samples were collected on a cold trap and subsequently transferred to the GC×GC system. For identification by GC×GC–TOF MS, a number of samples were collected and stored in tubes filled with a combination of Tenax TA, Carbopack B and Carboxen 1000 sorbents. Separation was performed using a 30 m×0.25 mm I.D.×1 μm DB-5 column in the first, and a 1 m×0.1 mm I.D.×0.1 μm Carbowax column in the second dimension and cryogenic jet-type modulation [62].

A rapid glance at Fig. 23 already reveals that more than two hundred peaks can be recognised in the chromatogram and that a 1D-GC run will, indeed, provide insufficient separation, with direct consequences for identification and quantification. However, the chromatogram contains many small peaks which are not immediately visible due to the limited dynamic range of the colours used to indicate peak intensity. Therefore, the total number of peaks can be expected to be much higher and is probably on the order of, at least, 500. Even though it is not immediately obvious because of the wide chemical variety of the compounds showing up, also in this chromatogram there is a 'hidden' ordered structure. For example, in the part of the chromatogram enlarged in insert A, many C_3-benzenes and closely related compounds are seen to elute, e.g. propyl-, methyl-ethyl-, and trimethylbenzenes. The peak assignment is based on identification by GC×GC–TOF MS and first-dimension linear RIs [62]. By using these data, 150 peaks could be identified in the in situ GC×GC–FID chromatogram. The majority of the analytes were hydrocarbons (alkanes, alkenes and benzenes); other substance classes were alcohols, aldehydes, ketones, nitriles and halogenated compounds.

The shot of Fig. 24, which shows a part of the chromatogram of Fig. 23, should serve as an illustration of the merits of a 3D presentation of the results of a GC×GC run. No doubt, many workers will appreciate such a presentation which, however, will display its real potential only when it is possible to view the 3D plot in a more interactive way (i.e. by changing the 'camera' position and view angle, and the scale of the *x*, *y* and *z* axes). The 3D view of Fig. 24 was generated by raytracing algorithms and required a calculation time of 1–2 min, which is much too long for such an interactive presentation.

As regards Fig. 24, there were, typically, only three modulations across a peak, i.e. only three data points were recorded in the first dimension. In order to generate a smooth surface, interpolation had to be performed; the resulting 3D view therefore does not reproduce the GC×GC data as precisely as one would desire.

3.9. PAHs in sediment: GC×GC–TOF MS

From a regulatory point of view, the polycyclic aromatic hydrocarbons (PAHs) are one of the most important classes of organic microcontaminants. Their presence can be due, e.g. oil spills, the incomplete combustion of wood or petrochemical

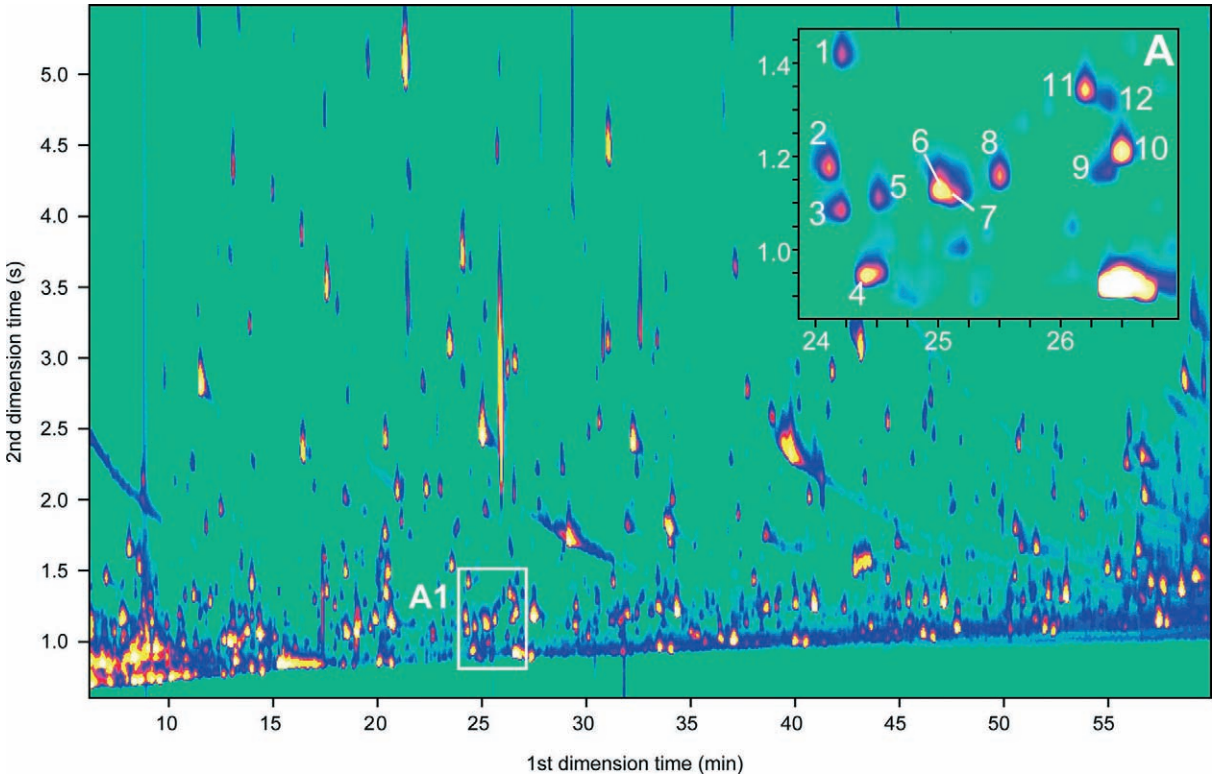

Fig. 23. GC×GC–FID chromatogram of air sample taken at Finokalia (Crete, Greece) using a DB-5×Carbowax column combination and a four-jet cryogenic modulator. Insert A is blow-up of area A1. Peaks: (based on GC×GC–TOF MS and RI): 1=(*Z*)-2-heptenal; 2=2-propenylbenzene; 3=2-ethylhexanal; 4=4-ethyloctane; 5=propylbenzene; 6=1-ethyl-3-methylbenzene; 7=1-ethyl-4-methylbenzene; 8=1,3,5-trimethylbenzene; 9=1-ethyl-2-methylbenzene; 10=2-octanone; 11=6-methyl-5-hepten-2-one; 12=methylstyrene.

products, and/or leaching from automobile tires. Concern about PAHs as environmental pollutants stems from the acute toxicity of 2- and 3-ring compounds such as anthracene and phenanthrene and the chronic toxicity (especially carcinogenicity) of some of the higher-molecular-mass compounds.

A sediment sample from the river Vistula (Poland) was extracted using 40-min pressurised hot-water extraction at 118 bar and 325 °C. The toluene extract was analysed by GC×GC–TOF MS with a 15 m×0.25 mm I.D.×0.25 μm DB-1 column in the first, and a 0.8 m×0.1 mm I.D.×0.1 μm BPX-50 column in the second dimension. The sample was found to contain a high concentration of saturated hydrocarbons, which show up as a horizontal band in the lower right-hand part of the GC×GC plot of Fig. 25. Next to these, there were also many compounds that were tentatively identified as derivatives of biphenylmethane and triphenylethane, i.e. compounds with two or three noncondensed benzene rings. The sample also contained many (alkyl-substituted) PAHs, though at lower concentrations. In Fig. 25, these are indicated by polygons, with dots showing the apices of peaks identified by the TOF MS data processing. As expected, the second-dimension retention time of the PAHs increases with the number of aromatic rings due to the stronger π–π interaction with the phenylene groups of the stationary phase (BPX-50) in the second column. Further, a number of aromatic sulphur-containing (e.g. benzothiophenes

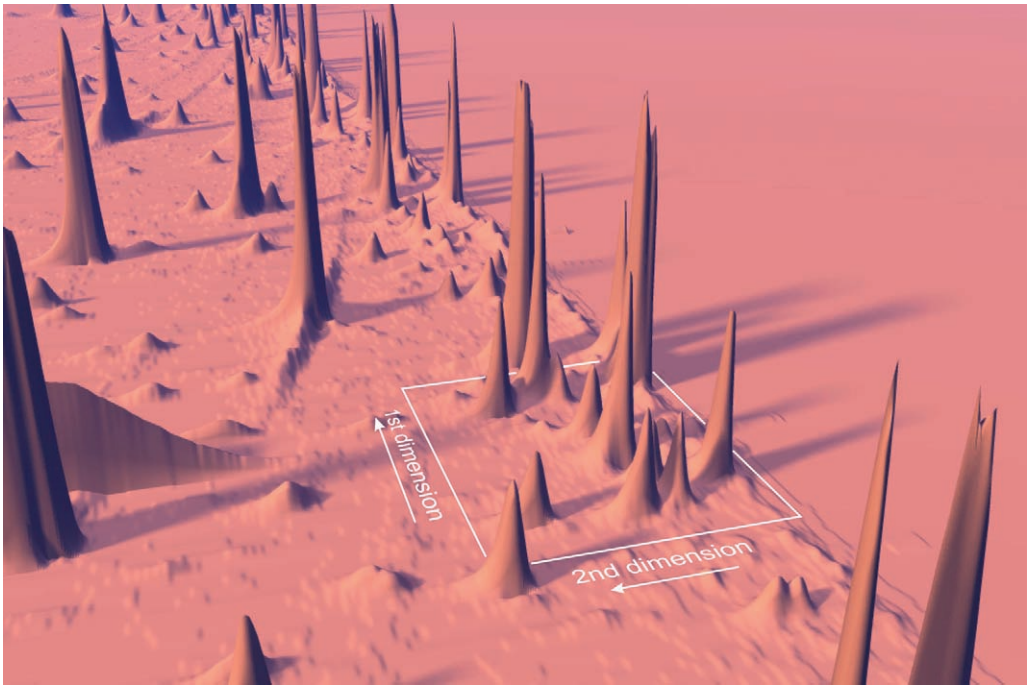

Fig. 24. 3D view of part of the GC×GC–FID chromatogram of Fig. 23. Rectangle is same part as shown in insert A of Fig. 23.

and dibenzothiophene) and nitrogen-containing (e.g. carbazole) compounds were identified on the basis of their mass spectra; some of them are indicated in Fig. 25.

3.10. Garlic powder: GC×GC–FID

The analysis of flavours and fragrances is a challenging task for the food chemist. Firstly, it is necessary to detect ultra-small amounts of compounds that contribute to the aroma in an often very complex matrix. These flavours usually comprise a wide range of classes of chemical compounds. Consequently, several papers have already been published which deal with the analysis of flavours in food, food ingredients and essential oils by means of GC×GC [29–31,35,86–90]. The application presented here is one typical example that should demonstrate the potential of GC×GC.

An SPME extract of the headspace of garlic powder was analysed by GC×GC–FID using a HP-1×BPX-50 column combination. The columns were temperature programmed from 30 °C (2 min hold) at 4 °C/min to 220 °C (5 min hold) [35]. The sample was also analysed on a GC×GC–TOF MS system with the same column combination for peak identification.

The 2–25-min part of the chromatogram of Fig. 26 is dominated by a number of intense peaks. Several of these (1–7) were identified by means of TOF MS; the peak identification is given in the legend to the figure. Due to peak tailing in the second dimension—which was probably caused by the rather high concentrations of these compounds—the peaks are longer than is usual. Surprisingly, even in the seemingly not very complex part at the right-hand side, indicated as B1, quite a number of peaks coelute in the first dimension. This becomes evident from insert B where a different shading was used for the colours indicating the peak intensity. Many peaks which are not visible in the larger 2D plot, now show up and reveal that the chromatogram is much more complex than expected at a first glance. This is

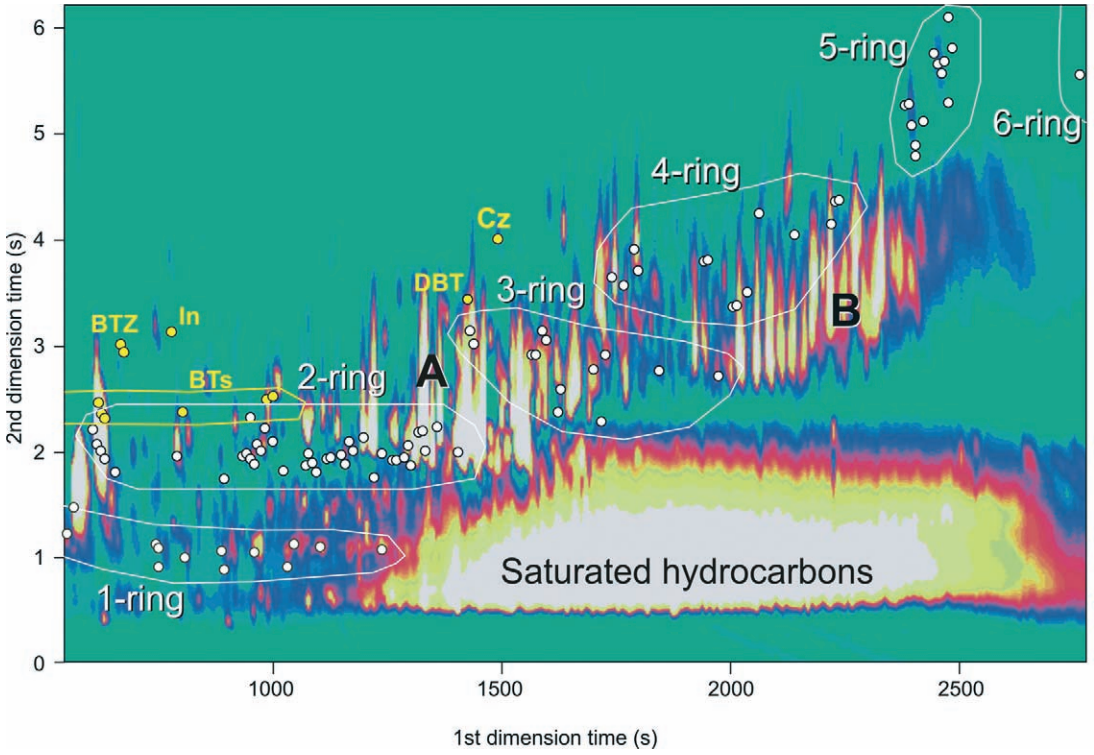

Fig. 25. GC×GC–TOF MS of a river sediment extract using a DB-1×BPX-50 column combination and an LMCS. Clusters of alkyl-substituted 1–6 ring PAHs are indicated by polygons. The groups of peaks indicated by A and B were tentatively identified as aromatic compounds containing two or three noncondensed benzene rings. Peaks: BTZ = benzothiazole; BTs = benzothiophenes; Cz = Carbazol; DBT = dibenzothiophene; In = indole.

another example of the care one should take when selecting a range of colours for producing a truly representative GC×GC chromatogram (see also Sections 2.6.1. and 3.8). It is our experience that two complementary ranges are often needed to retrieve all information stored in the chromatogram.

4. Conclusions

The main message that we want to deliver in the present overview is that GC×GC is, today, a powerful and versatile technique that can be used—and has, indeed, already been used—for the analysis of a wide variety of very complex samples. Here, one should add that the technique also improves the analysis of what are commonly called less complex samples: often, many more sample constituents are revealed than were, earlier, found with 1D-GC. Overall, the introduction of TOF MS for detection has, no doubt, been the major step forward in recent years: identification and confirmation of identity of target and nontarget analytes can now be carried out with relative ease.

With the principles (e.g. modulation, orthogonality, wrap-around) and the analytical strategies (e.g. the use of ordered structures, apex plots and deconvolution) of the technique being well understood, and analytical performance data being generated which are of high quality, there are no real barriers anymore for newcomers to the field, to start using GC×GC in research and development studies. Even so, it is prudent to quickly summarise the main advantages and present limitations of a GC×GC system-cum-operation.

One main advantage of most GC×GC applications is that the first-dimension column can be the same as, or closely similar to, the capillary GC

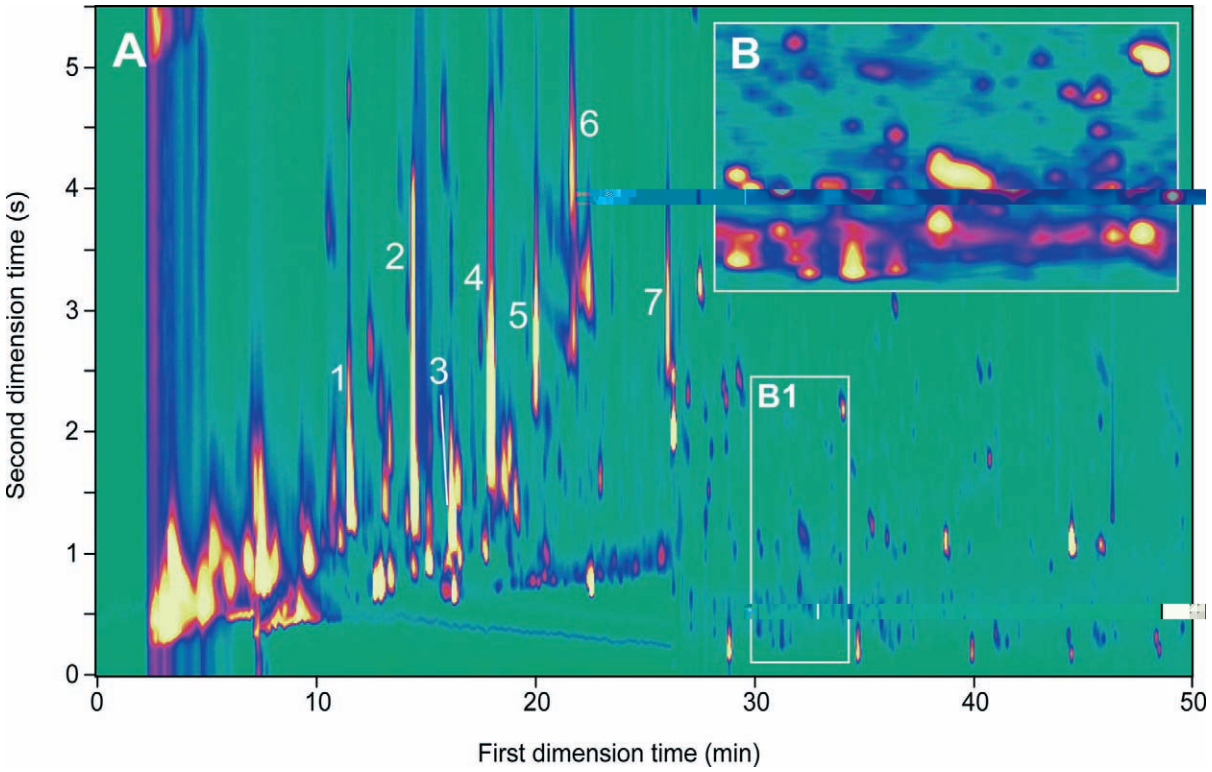

Fig. 26. (A) GC×GC–FID chromatogram of a SPME injection of a headspace sample of garlic powder using a 30 m, 0.32 mm I.D. HP-1×1.5 m, 0.1 mm I.D. BPX-50 column combination and a laboratory-made cryogenic modulator. (B) Blow-up of B1 (*x* axis five-fold enlarged). Peaks: 1=methyl-2-propenyl disulphide; 2=dimethyl trisulphide; 3=*m*-cymene; 4=diallyl disulphide; 5=methyl-2-propenyl trisulphide; 6=3-vinyl-1,2-dithiocyclohex-4-ene; 7=diallyl trisulphide.

column typically used for that application in 1D-GC. As a consequence, there is no limitation with regard to injection or (on-line) sample preparation techniques that can be used, which may—in the near future —also include on-line size-exclusion chromatography (SEC) or NPLC, i.e. SEC–GC×GC and NPLC–GC×GC. In addition, the newest generation of, mostly jet-type, cryogenic modulators is user-friendly and robust and there is little restriction as regards the application (i.e. analyte boiling-point) range. Next, experience shows that there are no real problems with finding a suitably polar second-dimension column to create the required orthogonal conditions. On the other hand, it has to be admitted that too little attention has been devoted so far to optimizing nonpolar×polar combinations for a variety of applications, and much more work can expected in this area. More importantly, the 100-μm I.D. second-dimension columns used in most publications, require relatively long, e.g. 4–10 s, second-dimension run times. Consequently, either under-sampling in the first dimension is tolerated (only 2–3 modulations across a peak) or slow temperature-programming rates of only 1–2 °C are used in the first dimension, causing run times to become considerably longer than is usual in 1D-GC. Fortunately, recently polar 50-μm I.D. columns became available which offer a much faster separation in the second dimension of a mere 1–2 s. A 3–4-fold lower total run time, a more optimised first-dimensional separation and a corresponding increase in signal intensity can now be achieved without adverse effects on modulation [34].

As regards detection, from the early days of GC×

GC, the FID has shown itself to be an excellent choice for all general-purpose work and, specifically in the predominant field of application, the analysis of petrochemical samples. As for the ECD, which probably is the most widely used selective detector in GC analysis because of the abundance of (poly-)-chlorinated organic microcontaminants present in environmental and biota samples, it can be used without significant problems if the internal volume is small enough and the auxiliary flow is sufficiently high [40,58]. The potential and performance of high-acquisition-rate (and, therefore, conventional resolution) TOF MS have been praised in several recent papers, and there is no need for repetition here. On the other hand, it is of interest to add that preliminary results were recently reported for two more detectors, the sulphur chemiluminescence detector [107] and the atomic emission detector [108]. In other words, additional selectivity in detection for GC×GC can be expected in the near future.

For the rest, there is—to our opinion—one pressing need, viz. the development of user-friendly software for quantification and the handling of retention windows. Also, while GC×GC–TOF MS provides unparalleled separation and identification power, the huge amount of information that is obtained requires new strategies for data processing and data reduction, and software tools to efficiently handle and automatedly process such data sets are urgently required. Actually, as we recently argued in another paper [60], even when these demands will have been met, it will not be possible to perform the most challenging analytical task—the recognition and identification of (large numbers of) nontarget analytes in very complex samples—in a fully automated fashion. Some manual processing and the dedicated use of chemical logic and the knowledge of an experienced analyst will still be required.

Finally, although it may sound somewhat premature: do we need further improvement of the present-day GC×GC separation procedures, frequently called ‘impressive’ or ‘unparalleled’ in the published literature? One glance at chromatograms such as one displayed in Figs. 10, 13, 23 and 25 of this paper makes it clear that the answer is affirmative. To our opinion, two approaches are promising. On the one hand, the combination with liquid-based separations such as SEC–GC×GC mentioned above, should be given careful attention, especially because of the different separation mechanism introduced in the first step. On the other hand, the GC-orientated approach should be further developed. One solution could be a GC×GC×GC system [109] which features three different separation mechanisms—and will, also, immediately require completely novel strategies with regard to data visualisation and processing. Another interesting approach, that has already been studied, uses two parallel columns of different polarity in the second dimension, i.e. GC×2GC [94]. One thing is certain here: having finally partly resolved what was, always, a structurless and huge background in too many chromatograms, analytical chemists will continue to apply more and more powerful additional techniques to unravel the composition of those bands and zones in their chromatograms that still defy proper identification today.

Acknowledgements

We are most grateful to Dr. G.J.M. Versteegh from the Netherlands Institute for Sea Research (Texel, The Netherlands) for the algae sample, technical assistance and valuable comments. We want to thank Mr. B. van der Horst from the Institute for Environmental Studies (Vrije Universiteit) who kindly provided the fly ash sample. Dr. J. Williams and Dr. Xu from the Max Planck Institute for Chemistry, Air Chemistry Department (Mainz, Germany) are gratefully acknowledged for their GC×GC data of the air samples. We thank Dr. A. de Kok, General Inspectorate for Health Protection (Amsterdam, the Netherlands) for the pesticide standard and the leek sample an Dr. T. Hyötyläinen (University of Helsinki, Finland) for the sediment sample. Our colleagues from the Vrije Universiteit L.L.P. van Stee, M. Adahchour and E.M. Kristenson, and Dr. J. Blomberg (Shell International Chemicals, Amsterdam, The Netherlands) are kindly acknowledged for their technical assistance and valuable discussions.

References

[1] G. Schomburg, J. Chromatogr. A 703 (1995) 309.
[2] W. Bertsch, J. High Resolut. Chromatogr. 22 (1999) 647.

[3] J.B. Phillips, J.Z. Xu, J. Chromatogr. A 703 (1995) 327.
[4] J.B. Phillips, J. Beens, J. Chromatogr. A 856 (1999) 331.
[5] H.-J. de Geus, U.A.Th. Brinkman, Trends Anal. Chem. 15 (1996) 168.
[6] Z. Liu, M.L. Lee, J. Microcol. Sep. 12 (2000) 241.
[7] W. Bertsch, J. High Resolut. Chromatogr. 23 (2000) 167.
[8] P.J. Marriott, R. Shellie, Trends Anal. Chem. 21 (2002) 573.
[9] R.C.Y. Ong, P.J. Marriott, J. Chromatogr. Sci. 40 (2002) 276.
[10] M. Pursch, K. Sun, B. Winniford, H. Cortes, A. Weber, T. McCabe, J. Luong, Anal. Bioanal. Chem. 373 (2002) 356.
[11] C.J. Venkatramani, J.B. Phillips, J. Microcol. Sep. 5 (1993) 511.
[12] J. Blomberg, P.J. Schoenmakers, J. Beens, R. Tijssen, J. High Resolut. Chromatogr. 20 (1997) 539.
[13] R.B. Gaines, G.S. Frysinger, M.S. Hendrick-Smith, J.D. Stuart, Environ. Sci. Technol. 33 (1999) 2106.
[14] P.J. Schoenmakers, J.L.M.M. Oomen, J. Blomberg, W. Genuit, G. van Velzen, J. Chromatogr. A 892 (2000) 29.
[15] C.J. Venkatramani, J.Z. Xu, J.B. Phillips, Anal. Chem. 68 (1996) 1486.
[16] R.E. Murphy, M.R. Schure, J.P. Foley, Anal. Chem. 70 (1998) 1585.
[17] J.V. Seeley, J. Chromatogr. A 962 (2002) 21.
[18] A.L. Lee, C.A. Lewis, K.D. Bartle, J.B. McQuaid, P.J. Marriott, J. Microcol. Sep. 12 (2000) 187.
[19] J. Beens, M. Adahchour, R.J.J. Vreuls, K. van Altena, U.A.Th. Brinkman, J. Chromatogr. A 919 (2001) 127.
[20] R.M. Kinghorn, P.J. Marriott, J. High Resolut. Chromatogr. 22 (1999) 235.
[21] J. Dallüge, R.J.J. Vreuls, J. Beens, U.A.Th. Brinkman, J. Sep. Sci. 25 (2002) 201.
[22] R. Ong, P.J. Marriott, P. Morrison, P. Haglund, J. Chromatogr. A 962 (2002) 135.
[23] P. Haglund, M. Harju, C. Danielsson, P.J. Marriott, J. Chromatogr. A 962 (2002) 127.
[24] J. Beens, R. Tijssen, J. Blomberg, J. Chromatogr. A 822 (1998) 233.
[25] J.C. Giddings, J. Chromatogr. A 703 (1995) 3.
[26] H.-J. de Geus, I. Aidos, J. de Boer, J.B. Luten, U.A.Th. Brinkman, J. Chromatogr. A 910 (2001) 95.
[27] P. Korytár, P.E.G. Leonards, J. de Boer, U.A.Th. Brinkman, J. Chromatogr. A 958 (2002) 203.
[28] P. Haglund, M. Harju, R. Ong, P.J. Marriott, J. Microcol. Sep. 13 (2001) 306.
[29] R. Shellie, P.J. Marriott, C. Cornwell, J. Sep. Sci 24 (2001) 823.
[30] R. Shellie, P.J. Marriott, Anal. Chem. 74 (2002) 5426.
[31] R. Shellie, P.J. Marriott, P. Morrison, Anal. Chem. 73 (2001) 1336.
[32] J. Beens, J. Blomberg, P.J. Schoenmakers, J. High Resolut. Chromatogr. 23 (2000) 182.
[33] J. Dallüge, M. van Rijn, J. Beens, R.J.J. Vreuls, U.A.Th. Brinkman, J. Chromatogr. A 965 (2002) 207.
[34] M. Adahchour, A. Taşoz, J. Beens, R.J.J. Vreuls, A.M. Batenburg, U.A.Th. Brinkman, J. Sep. Sci.. in press.
[35] M. Adahchour, J. Beens, R.J.J. Vreuls, A.M. Batenburg, E.A.E. Rosing, U.A.Th. Brinkman, Chromatographia 55 (2002) 361.
[36] R.B. Gaines, E.B. Ledford, J.D. Stuart, J. Microcol. Sep. 10 (1998) 597.
[37] Z.Y. Liu, J.B. Phillips, J. Chromatogr. Sci. 29 (1991) 227.
[38] J.B. Phillips, R.B. Gaines, J. Blomberg, F.W.M. van der Wielen, J.M. Dimandja, V. Green, J. Granger, D. Patterson, L. Racovalis, H.-J. de Geus, J. de Boer, P. Haglund, J. Lipsky, V. Sinha, E.B.A. Ledford, J. High Resolut. Chromatogr. 22 (1999) 3.
[39] P.J. Marriott, R.M. Kinghorn, R. Ong, P. Morrison, P. Haglund, M. Harju, J. High Resolut. Chromatogr. 23 (2000) 253.
[40] H.-J. de Geus, A. Schelvis, J. de Boer, U.A.Th. Brinkman, J. High Resolut. Chromatogr. 23 (2000) 189.
[41] P.J. Marriott, R.M. Kinghorn, Trends Anal. Chem. 18 (1999) 114.
[42] P.J. Marriott, R.M. Kinghorn, J. Chromatogr. A 866 (2000) 203.
[43] R.M. Kinghorn, P.J. Marriott, J. High Resolut. Chromatogr. 21 (1998) 620.
[44] P.J. Marriott, R.M. Kinghorn, Anal. Sci. 14 (1998) 651.
[45] R.M. Kinghorn, P.J. Marriott, P.A. Dawes, J. High Resolut. Chromatogr. 23 (2000) 245.
[46] E.B. Ledford, C.A. Billesbach, J.R. Termaat, Int. Pat. PCT/US01/01065 (2001)
[47] P. Korytár, L.R. Bordajandi, P.E.G. Leonards, J. de Boer, U.A.Th. Brinkman, in preparation.
[48] M. Adahchour, J. Beens, U.A.Th. Brinkman, in preparation.
[49] C.A. Bruckner, B.J. Prazen, R.E. Synovec, Anal. Chem. 70 (1998) 2796.
[50] C.G. Fraga, B.J. Prazen, R.E. Synovec, Anal. Chem. 72 (2000) 4154.
[51] J.V. Seeley, F. Kramp, C.J. Hicks, Anal. Chem. 72 (2000) 4346.
[52] H.-J. de Geus, J. de Boer, U.A.Th. Brinkman, J. Chromatogr. A 767 (1997) 137.
[53] E.B. Ledford, C.A. Billesbach, J. High Resolut. Chromatogr. 23 (2000) 202.
[54] T. Hyötyläinen, M. Kallio, K. Hartonen, M. Jussila, S. Palonen, M.-L. Riekkola, Anal. Chem. 74 (2002) 4441.
[55] J. Beens, J. Dallüge, M. Adahchour, R.J.J. Vreuls, U.A.Th. Brinkman, J. Microcol. Sep. 13 (2001) 134.
[56] J. Harynuk, T. Górecki, J. Sep. Sci. 25 (2002) 304.
[57] J. Beens, H. Boelens, R. Tijssen, J. Blomberg, J. High Resolut. Chromatogr. 21 (1998) 47.
[58] E.M. Kristenson, P. Korytár, C. Danielsson, M. Kallio, R.J.J. Vreuls, J. Beens, U.A.Th. Brinkman, in preparation.
[59] M. van Deursen, J. Beens, J. Reijenga, P. Lipman, C.A. Cramers, J. Blomberg, J. High Resolut. Chromatogr. 23 (2000) 507.
[60] J. Dallüge, L.L.P. van Stee, X. Xu, J. Williams, J. Beens, R.J.J. Vreuls, U.A.Th. Brinkman, J. Chromatogr. A 974 (2002) 169.
[61] R. Shellie, L.-L. Xie, P.J. Marriott, J. Chromatogr. A 968 (2002) 161.
[62] X. Xu, J.Williams, J. Lelieveld, L.L.P. van Stee, J. Beens, R.J.J. Vreuls, U.A.Th. Brinkman, Atmos. Chem. Phys., submitted for publication.

[63] R.J. Western, P.J. Marriott, J. Sep. Sci. 25 (2002) 832.
[64] G.S. Frysinger, R.B. Gaines, E.B. Ledford, J. High Resolut. Chromatogr. 22 (1999) 195.
[65] G.S. Frysinger, R.B. Gaines, J. High Resolut. Chromatogr. 23 (2000) 197.
[66] A.L. Lee, K.D. Bartle, A.C. Lewis, Anal. Chem. 73 (2001) 1330.
[67] H.-J. de Geus, J. de Boer, J.B. Phillips, E.B. Ledford, U.A.Th. Brinkman, J. High Resolut. Chromatogr. 21 (1998) 411.
[68] P.J. Marriott, R.C.Y. Ong, R.M. Kinghorn, P.D. Morrison, J. Chromatogr. A 892 (2000) 15.
[69] S.E. Reichenbach, M. Ni, D. Zhang, E.B. Ledford, in: Proc. 25th Intern. Symp. Cap. Chromatogr., Riva del Garda, Italy, 2002.
[70] E. Sánchez, L.S. Ramos, B.R. Kowalski, J. Chromatogr. 385 (1987) 152.
[71] C.G. Fraga, B.J. Prazen, R.E. Synovec, J. High Resolut. Chromatogr. 23 (2000) 215.
[72] K.J. Johnson, B.J. Prazen, R.K. Olund, R.E. Synovec, J. Sep. Sci. 25 (2002) 297.
[73] B.J. Prazen, C.A. Bruckner, R.E. Synovec, B.R. Kowalski, J. Microcol. Sep. 11 (1999) 97.
[74] C.G. Fraga, B.J. Prazen, R.E. Synovec, Anal. Chem. 73 (2001) 5833.
[75] C.G. Fraga, C.A. Bruckner, R.E. Synovec, Anal. Chem. 73 (2001) 675.
[76] B.J. Prazen, K.J. Johnson, A. Weber, R.E. Synovec, Anal. Chem. 73 (2001) 5677.
[77] M. van Deursen, Novel concepts for fast capillary gas chromatography, Ph. D. Dissertation, Technische Universiteit Eindhoven, 2002, Universiteitsdrukkerij, Eindhoven.
[78] J. Blomberg, Multidimensional GC-based separations for the oil and petrochemical industry, Ph.D. Dissertation, Vrije Universiteit Amsterdam, 2002, Universal Press, Veenendaal.
[79] J. Beens, Chromatographic couplings for unraveling oil fractions, Ph.D. Dissertation, University of Amsterdam, 1998, Universal Press, Veenendaal.
[80] J. Beens, U.A.Th. Brinkman, Trends Anal. Chem. 19 (2000) 260.
[81] K.J. Johnson, R.E. Synovec, Chemom. Intell. Lab. Syst. 60 (2002) 225.
[82] G.S. Frysinger, R.B. Gaines, J. High Resolut. Chromatogr. 22 (1999) 251.
[83] G.S. Frysinger, R.B. Gaines, J. Sep. Sci. 24 (2001) 87.
[84] G.S. Frysinger, R.B. Gaines, J. Forens. Sci. 47 (2002) 471.
[85] G.S. Frysinger, R.B. Gaines, C.M. Reddy, Env. Forens. 3 (2002) 27.
[86] P.J. Marriott, R. Shellie, J. Fergeus, R. Ong, P. Morrison, Flav. Fragr. J. 15 (2000) 225.
[87] R. Shellie, P.J. Marriott, C. Cornwell, J. High Resolut. Chromatogr. 23 (2000) 554.
[88] J.M.D. Dimandja, S.B. Stanfill, J. Grainger, D.G. Patterson, J. High Resolut. Chromatogr. 23 (2000) 208.
[89] P.J. Marriott, R. Shellie, C. Cornwell, J. Chromatogr. A 936 (2001) 1.
[90] R. Shellie, L. Mondello, P.J. Marriott, G. Dugo, J. Chromatogr. A 970 (2002) 225.
[91] M. Harju, P. Haglund, J. Microcol. Sep. 13 (2001) 300.
[92] P. Korytár, L.L.P. van Stee, P.E.G. Leonards, J. de Boer, U.A.Th. Brinkman, J. Chromatogr. A, submitted for publication.
[93] R.J. Western, S.S.G. Lau, P.J. Marriott, P.D. Nichols, Lipids 37 (2002) 715.
[94] Z.Y. Liu, S.R. Sirimanne, D.G. Patterson, L.L. Needham, J.B. Phillips, Anal. Chem. 66 (1994) 3086.
[95] J.V. Seeley, F.J. Kramp, K.S. Sharpe, J. Sep. Sci. 24 (2001) 444.
[96] J.V. Seeley, F.J. Kramp, K.S. Sharpe, S.K. Seeley, J. Sep. Sci. 25 (2002) 53.
[97] A.C. Lewis, N. Carslaw, P.J. Marriott, R.M. Kinghorn, P. Morrison, A.L. Lee, K.D. Bartle, M.J. Pilling, Nature 405 (2000) 778.
[98] K. Sun, B.L. Winniford, J. Luong, H. Cortes, B. Gerhart, J. Griffith, R. Shellie, P.J. Marriott, in: Proc. 25th Intern. Symp. Cap. Chromatogr., Riva del Garda, 2002.
[99] P.J. Marriott, O. Trapp, R. Shellie, V. Schurig, J. Chromatogr. A 919 (2001) 115.
[100] R. Ong, R. Shellie, P.J. Marriott, J. Sep. Sci. 24 (2001) 367.
[101] J. Beens, R. Tijssen, J. Microcol. Sep. 7 (1995) 345.
[102] I. Dzidic, H.A. Petersen, P.A. Wadsworth, H.V. Hart, Anal. Chem. 64 (1992) 2227.
[103] H. Schulz, W. Böhringer, P. Waller, F. Ousmanov, Catal. Today 49 (1999) 87.
[104] P. Steketee, I. Freriks, M. Schrap, R. Faasen, Honderden bestrijdingsmiddelen, RIZA Report 2000.020, Lelystad, The Netherlands, 2000.
[105] J.K. Volkman, S.M. Barrett, S.I. Blackburn, M.P. Mansour, E.L. Sikes, F. Gelin, Org. Geochem. 29 (1998) 1163.
[106] M. van den Berg, L. Birnbaum, A.T.C. Bosveld, B. Brunstrom, P. Cook, M. Feeley, J.P. Giesy, A. Hanberg, R. Hasegawa, S.W. Kennedy, T. Kubiak, J.C. Larsen, F.X.R. van Leeuwen, A.K.D. Liem, C. Nolt, R.E. Peterson, L. Poellinger, S. Safe, D. Schrenk, D. Tillitt, M. Tysklind, M. Younes, F. Waern, T. Zacharewski, Environ. Health Perspect. 106 (1998) 775.
[107] J. Blomberg, in: Agilent GC seminar, Amstelveen, the Netherlands, 2002.
[108] L.L.P. van Stee, in: Annual meeting of the Netherlands Organisation for Scientific Research, Section Analytical Chemistry, Lunteren, the Netherlands, 2002.
[109] E.B. Ledford, C.A. Billesbach, Q. Zhu, J. High Resolut. Chromatogr. 23 (2000) 205.